TECTONICS, VOL. 32, 1247–1271, doi:10.1002/tect.20077, 2013

Early Cretaceous sedimentation and orogeny on the active margin of Eurasia: Southern Central Pontides, Turkey

Aral I. Okay,[1] Gürsel Sunal,[2] Sarah Sherlock,[3] Demir Altıner,[4] Okan Tüysüz,[1] Andrew R. C. Kylander-Clark,[5] and Mesut Aygül[1]

Received 23 December 2012; revised 18 August 2013; accepted 21 August 2013; published 1 October 2013.

[1] The Pontides in northern Turkey constituted part of the southern active margin of Eurasia during the Mesozoic. In the Early Cretaceous, a large submarine turbidite fan covered most of the Central Pontides. New U-Pb detrital zircon data imply that the major source of the turbidites was the East European Craton-Scythian Platform in the north. This implies that there was no thoroughgoing Black Sea basin between the Pontides and the East European Craton during the Early Cretaceous. The Lower Cretaceous turbidites are bounded in the south by a large metamorphic area, the Central Pontide Supercomplex (CPS). New geological mapping, petrology, and U-Pb zircon and Ar-Ar muscovite ages indicate that the northern part of the CPS consists of Lower Cretaceous distal turbidites deformed and metamorphosed in a subduction zone in the Albian. The rest of the CPS is made of Middle Jurassic, Lower Cretaceous, and middle Cretaceous (Albian) metamorphic belts, each constituting distinct subduction-accretion units. They represent episodes of collision of oceanic volcanic arcs and oceanic plateaus with the Eurasian margin and are marked in the stratigraphy of the hinterland by periods of uplift and erosion. The accretionary complexes are overlain by Upper Cretaceous (Turonian-Santonian) volcano-sedimentary sequences deposited in a fore-arc setting. The detrital zircon data, middle Cretaceous (Albian) metamorphism, and widespread Albian uplift of the Black Sea region suggest that Early Cretaceous (Barremian-Aptian) nonvolcanic rifting and Late Cretaceous (Turonian-Santonian) opening of the Black Sea by the splitting of the arc are unrelated events.

Citation: Okay, A. I., G. Sunal, S. Sherlock, D. Altıner, O. Tüysüz, A. R. C. Kylander-Clark, and M. Aygül (2013), Early Cretaceous sedimentation and orogeny on the active margin of Eurasia: Southern Central Pontides, Turkey, *Tectonics*, *32*, 1247–1271, doi:10.1002/tect.20077.

1. Introduction

[2] In active plate margins, the relationship between extension, contraction, sedimentary deposition, and metamorphism is often complex and changes both spatially and temporally. This is especially the case in regions where back-arc extension occurs during subduction. An example is the Black Sea-Pontide system, where subduction of the Tethyan ocean under the Pontides during the Cretaceous is linked to the opening of the Black Sea as a back-arc basin [e.g., *Boccaletti et al*., 1974; *Zonenshain and Le Pichon*, 1986; *Okay et al*., 1994; *Robinson et al*., 1996]. At present, a distance of ~100 km, corresponding to the width of the Pontide mountain chain, separates the undeformed Cretaceous to Recent sediments of the Black Sea basin from the İzmir-Ankara suture, representing the location of the former oceanic subduction zone (Figure 1). The Cretaceous rocks of the Pontides record both the extensional opening of the Black Sea in the north and the subduction-related shortening and metamorphism in the south. In this context, we have studied the relationship between deposition, contractional deformation, and metamorphism of an extensive Lower Cretaceous submarine turbidite sequence in the Central Pontides with outcrops extending from the Black Sea margin to the İzmir-Ankara suture (Figure 1). Through geological mapping, biostratigraphy, petrology, and zircon U-Pb and muscovite Ar-Ar geochronology, we show that deposition of the submarine turbidites in the north during the Early Cretaceous (Barremian-Aptian) was immediately followed and partly overlapped with their contractional deformation and metamorphism in the subduction zone in the south.

Additional supporting information may be found in the online version of this article.

[1]Eurasia Institute of Earth Sciences, Istanbul Technical University, Istanbul, Turkey.
[2]Faculty of Mines, Department of Geology, Istanbul Technical University, Istanbul, Turkey.
[3]Department of Earth, Environment and Ecosystems, Centre for Earth, Planetary, Space & Astronomical Research (CEPSAR) Sciences, The Open University, Milton Keynes, UK.
[4]Department of Geology, Middle East Technical University, Ankara, Turkey.
[5]Department of Earth Sciences, University of California, Santa Barbara, California, USA.

Corresponding author: A. I. Okay, Eurasia Institute of Earth Sciences, Istanbul Technical University, Maslak 34469, Istanbul, Turkey. (okay@itu.edu.tr)

0278-7407/13/10.1002/tect.20077

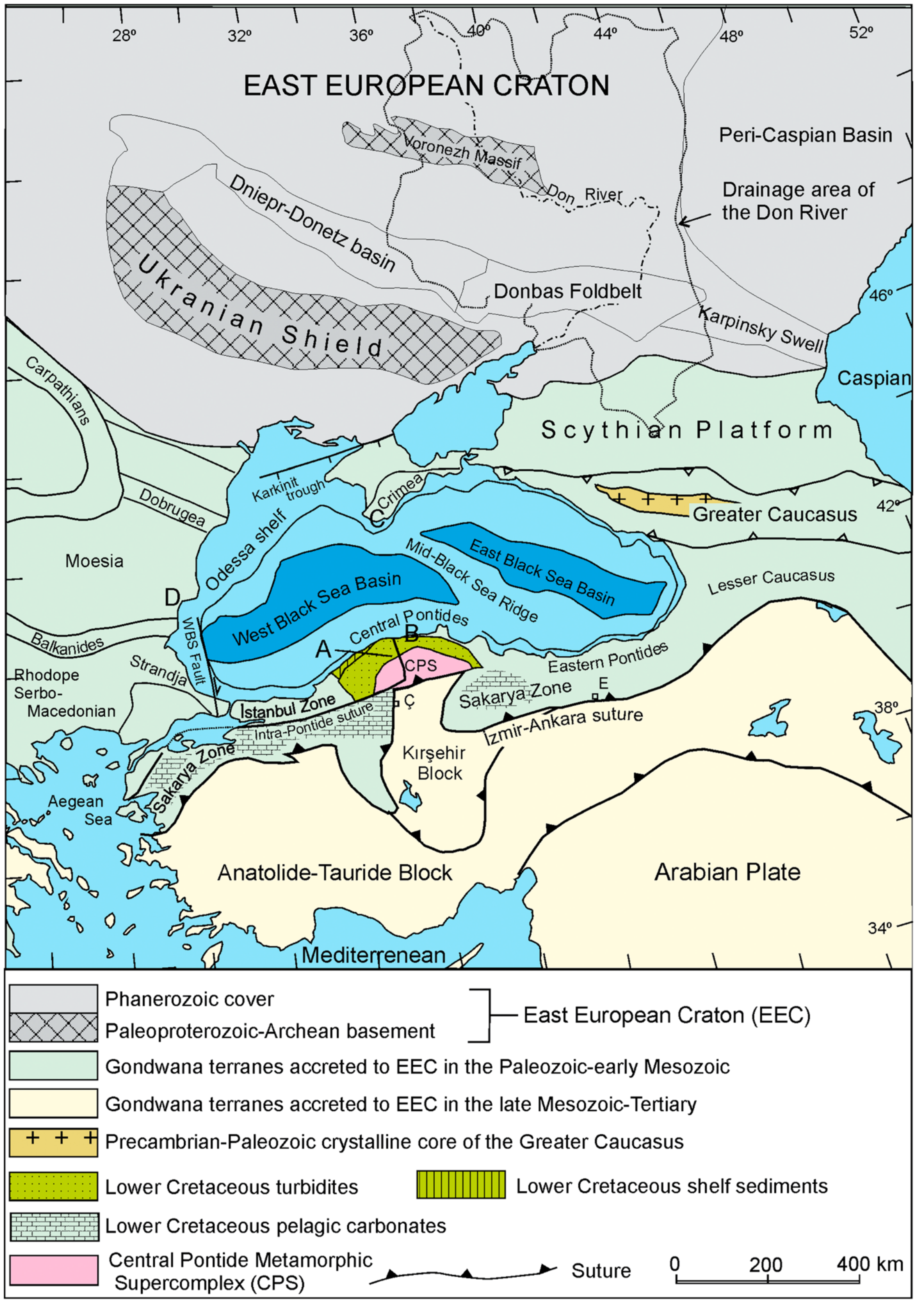

Figure 1. Tectonic map of the Eastern Mediterranean-Black Sea region. Abbreviations: CPS, Central Pontide Metamorphic Supercomplex; E, Erzincan; Ç, Çankırı; WBS Fault, West Back Sea Fault.

[3] Tectonic events in active continental margins, such as collisions with large oceanic edifices, lead to deformation and uplift in the continental hinterland and influence the sedimentation pattern. We explore this relation by comparing the ages of the subduction-accretion episodes of the Pontide margin with the sedimentation pattern in the Eurasian hinterland in the Black Sea region.

[4] The Black Sea basin with its >10 km thick sedimentary infill is an active area for hydrocarbon exploration, with several dry deep-sea wells opened recently by BP, Petrobras, ExxonMobil, Chevron, and Turkish Petroleum Corporation along the southern Black Sea margin (http://www.tpao.gov.tr/tp2/sub_en/sub_content.aspx?id=79). A major problem encountered in these wells has been the poor quality of potential sandstone reservoirs [e.g., *Vincent et al.*, 2013]. In this context, the source of the sandstones in the Black Sea basin, whether from the granitoids and gneisses of the East European Craton in the north or from the metamorphic and volcanic rocks from the Pontides, is a key issue. Here, we provide clastic zircon data from the Lower Cretaceous sandstones and Ar-Ar data from the metamorphic rocks, which point to the East European Craton as a major source for the Lower Cretaceous sandstones in the Black Sea region.

[5] The Central Pontides has been an important area for the development of the models and concepts related to the Paleo-Tethys [*Şengör et al.*, 1980, 1984; *Yılmaz and Şengör*, 1985; *Tüysüz*, 1990; *Tüysüz and Yiğitbaş*, 1994; *Ustaömer and Robertson*, 1994, 1997, 1999; *Yılmaz et al.*, 1997b].

In these studies, the large area of greenschist-facies to eclogite-facies metamorphic rocks in the southern part of the Central Pontides (Figure 1) has been considered to have formed during the Triassic subduction of the Paleo-Tethys. Through zircon U-Pb and mica Ar-Ar geochronology, we show here that the sedimentation and metamorphism in this region are of Early Cretaceous and Jurassic ages. This requires revision of the models related to the evolution of the Paleo-Tethys, including the prevalent concept of the Triassic Küre back-arc basin.

2. Geological Setting

[6] The Pontides is the mountain chain between the Black Sea and the Anatolide-Tauride and Kırşehir blocks in Turkey (Figure 1). The İzmir-Ankara suture, which separates the Pontides from the Anatolide-Tauride and Kırşehir blocks, represents the trace of a wide Tethyan ocean, which was finally closed through northward subduction during the latest Cretaceous to early Tertiary [*Şengör and Yılmaz*, 1981; *Okay and Tüysüz*, 1999; *Cavazza et al*., 2012]. Paleogeographically, the Pontides have been part of the southern margin of Eurasia at least since the Early Mesozoic [e.g., *Enay*, 1976; *Channel et al*., 1996].

[7] The Pontides consist of three terranes, which are the Sakarya and Istanbul zones, and the Strandja Massif [Figure 1; *Okay and Tüysüz*, 1999]. The Central Pontides is a loosely defined term describing the northward arched section of the Pontide mountain chain. It includes two of the Pontic terranes: the Istanbul Zone in the west and the Sakarya Zone in the east. In the northern part of the Central Pontides, an Upper Jurassic-Lower Cretaceous shallow marine carbonate sequence covers unconformably the units of the Istanbul and Sakarya zones (Figure 2), showing that they were amalgamated before the Late Jurassic [e.g., *Yiğitbaş et al*., 1999; Figures 2 and 3].

3. Lower Cretaceous Turbidites: The Çağlayan Formation

[8] Geological map of the Central Pontides, published by the Geological Survey of Turkey (Maden Tetkik ve Arama Enstitüsü, Ankara), shows large areas made up of “Upper Paleozoic-Triassic metamorphic rocks” [*Uğuz et al*., 2002]. However, our mapping has showed that large parts of these “metamorphic rocks” are constituted of Lower Cretaceous turbidites, which cover an area measuring 300 km by 60 km (Figures 1 and 2). They are often described as the Çağlayan Formation in the east and the Ulus Formation in the west [e.g., *Tüysüz*, 1999]. Both formations have a similar age and lithology, and the name Çağlayan Formation will be used here for all the Lower Cretaceous turbidites in the Central Pontides. Recent determination of nannofossils from an extensive sample set from the Çağlayan Formation by *Hippolyte et al*. [2010] produced predominantly Barremian to late Aptian ages, which are compatible with the earlier paleontological age data [*Gedik and Korkmaz*, 1984, *Tüysüz*, 1999]. The maximum thickness of the Çağlayan Formation is difficult to determine precisely because of deformation and because of its erosional upper boundary. Most estimates put it in the range of 2000–3000 m [*Aydın et al*., 1982; *Gedik and Korkmaz*, 1984; *Tüysüz*, 1999; *Hippolyte et al*., 2010]. The Ulus-1 well north of Karabük has penetrated 2850 m of the Çağlayan Formation [*Derman*, 2002], and the Boyabat-3 and Boyabat-4 wells north of Boyabat have gone through 3000 m of Lower Cretaceous turbidites [*Şen*, 2013]. The Çağlayan Formation continues north toward the Black Sea under the younger cover; the Soğuksu-1 well southeast of Ayancık (Figure 2) has cut through 1050 m of Lower Cretaceous turbidites under the Upper Cretaceous volcanic rocks [*Korkmaz*, 1992].

[9] The Çağlayan Formation rests unconformably on various basement units of the Istanbul and Sakarya zones, ranging from Neoproterozoic granites, Paleozoic and Triassic sedimentary rocks, Jurassic granitoids, and Upper Jurassic-Lower Cretaceous limestones [Figures 2 and 3; *Tüysüz*, 1999]. The youngest rocks below the Çağlayan Formation are shallow marine carbonates, which have a Kimmeridgian to Berriasian age range in the Central Pontides [*Tunoğlu*, 1991; *Derman*, 2002; our unpublished data]. This indicates significant uplift and erosion in the Early Cretaceous (Valanginian-Hauterivian) prior to the deposition of the Çağlayan Formation. The Çağlayan Formation is unconformably overlain by the Upper Cretaceous pelagic limestones [*Tüysüz*, 1999; *Okay et al*., 2006; *Hippolyte et al*., 2010].

[10] Outcrops of Barremian to Albian shallow marine carbonate, shale, and sandstone along the Black Sea coast between Zonguldak and Amasra delimit the northwestern margin of the Çağlayan basin [Figure 2; *Tüysüz*, 1999; *Yılmaz and Altıner*, 2007; *Masse et al*., 2009; *Hippolyte et al*., 2010]. Lower Cretaceous rocks are absent further west along the Black Sea margin. In the western Sakarya Zone, the Early Cretaceous (Berriasian-Aptian) is represented by pelagic carbonates [*Altıner et al*., 1991], which also extend further east toward the Eastern Pontides [Figure 1; *Rojay and Altıner*, 1998]. However, over most of the Eastern Pontides, the Aptian-Albian period is usually a hiatus in the stratigraphy [*Robinson et al*., 1995; *Okay and Şahintürk*, 1997]. The Çağlayan basin as used here is generally divided into an Ulus basin in the west and Sinop-Boyabat basin in the east; however, our mapping has shown that these basins are interconnected and form a single turbidite depocenter.

[11] Proximal to distal turbidites consisting of sandstone and dark shale are the most common sedimentary facies in the Çağlayan Formation [e.g., *Tüysüz*, 1999; *Hippolyte et al*., 2010]. They display typical turbidite features including Bouma sequences, graded bedding, flute casts, grooves, slump structures, etc. [e.g., *Aydın et al*., 1982; *Derman*, 2002]. The Çağlayan Formation also contains extensive mass flow horizons ranging from grain flows to olistostromes with clasts up to a few kilometers across [*Görür,* 1997]. The most common clasts are Upper Jurassic-Lower Cretaceous shallow marine limestone with lesser blocks of Paleozoic and Triassic sandstone and limestone, phyllite, and granitoid [*Tüysüz*, 1999; *Derman*, 2002]. Associated with the olistostromes are 100 m thick sequences of medium-bedded calciturbidite and shale. Toward the south, turbidites become more distal and are dominated by black shales with few and fine-grained sandstone and mass flow horizons.

[12] The olistoliths in the Çağlayan Formation are especially large and dense in the region between Azdavay and Küre (Figure 2). The allochthonous setting of the kilometer-size

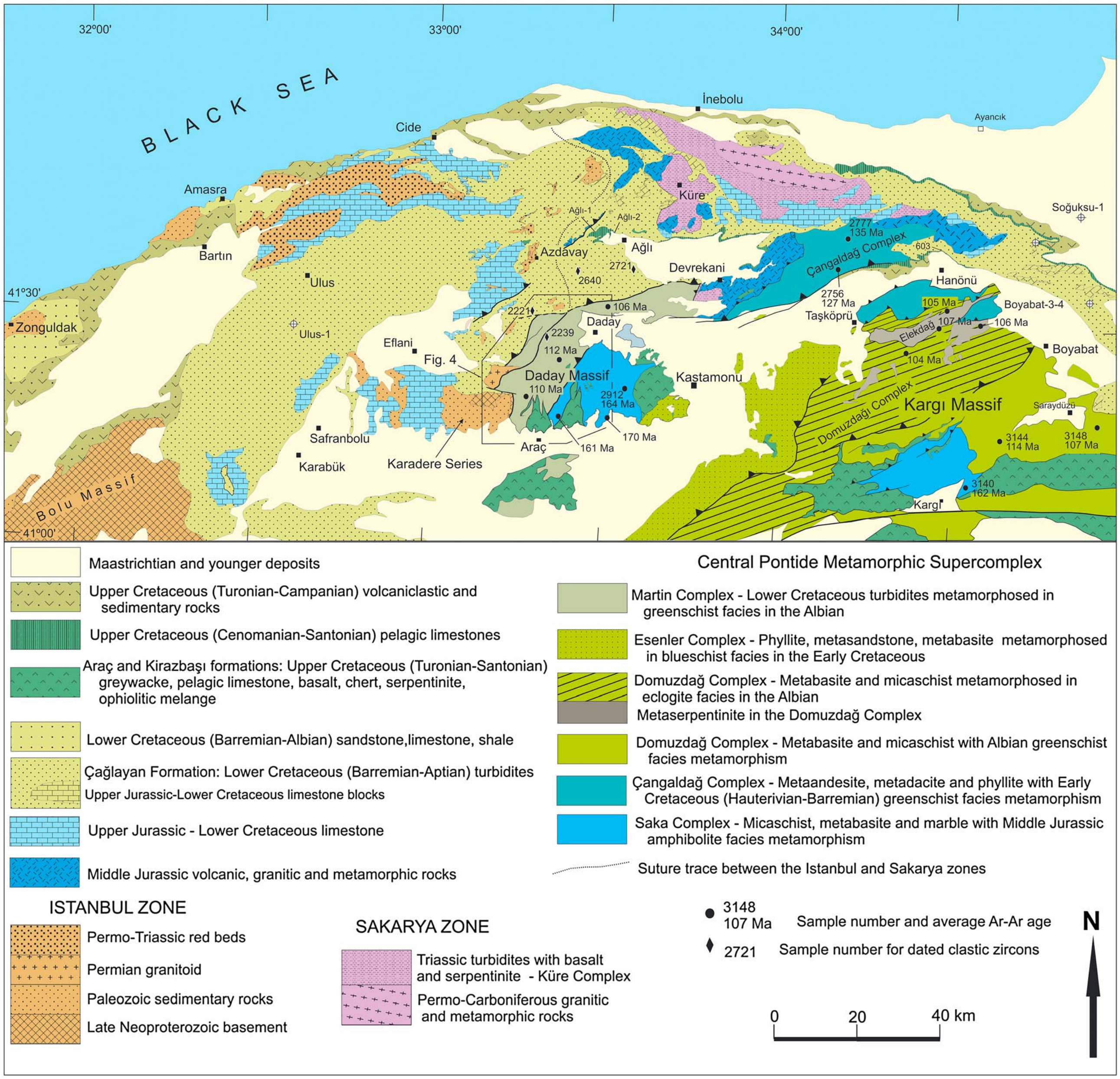

Figure 2. Geological map of the northern Central Pontides [compiled from *Aksay et al*., 2002; *Uğuz et al*., 2002 and this study].

blocks are proved by the exploratory coal wells drilled in the Carboniferous series in the Azdavay region. Several of the wells have passed through the Carboniferous and Triassic sequences and have entered Lower Cretaceous turbidites at depths of 100 to 500 m [*Canca*, 1994]. The olistoliths are associated with debris flows with the clasts ranging from a few centimeters to a hundred meters. The kilometer size of the olistoliths precludes long-distance transport. This is also shown by the observation that the Paleozoic-Triassic blocks are restricted to the western part of the Central Pontides (Figure 2). In the eastern Sakarya part of the Central Pontides, the olistoliths are predominantly Upper Jurassic-Lower Cretaceous limestone. Based on the paleostress studies in the Çağlayan Formation, *Hippolyte et al*. [2012] infer that the pre-Cretaceous substratum was disrupted and fragmented under ESE directed extension during the Barremian and Aptian. The large blocks must have slid from uplifted horsts into the adjacent basins, which had depths of over a kilometer. With these extensional features, the Çağlayan Formation is interpreted as the syn-rift deposits of the Black Sea basin [*Görür*, 1988, 1997].

[13] In terms of hydrocarbon potential, the Çağlayan Formation shows source, reservoir, and seal characteristics [*Aydın et al*., 1995; *Robinson et al*., 1996; *Görür and Tüysüz*, 1997; *Şen*, 2013], and there is one oil seep in the Çağlayan Formation north of Boyabat [*Derman and İztan*, 1997]. The shales of the Çağlayan Formation have variable total organic carbon contents ranging from 0.5 to 2.0 wt %. Several dry oil wells have been drilled in the Central Pontides targeting the Çağlayan Formation [*Şen*, 2013].

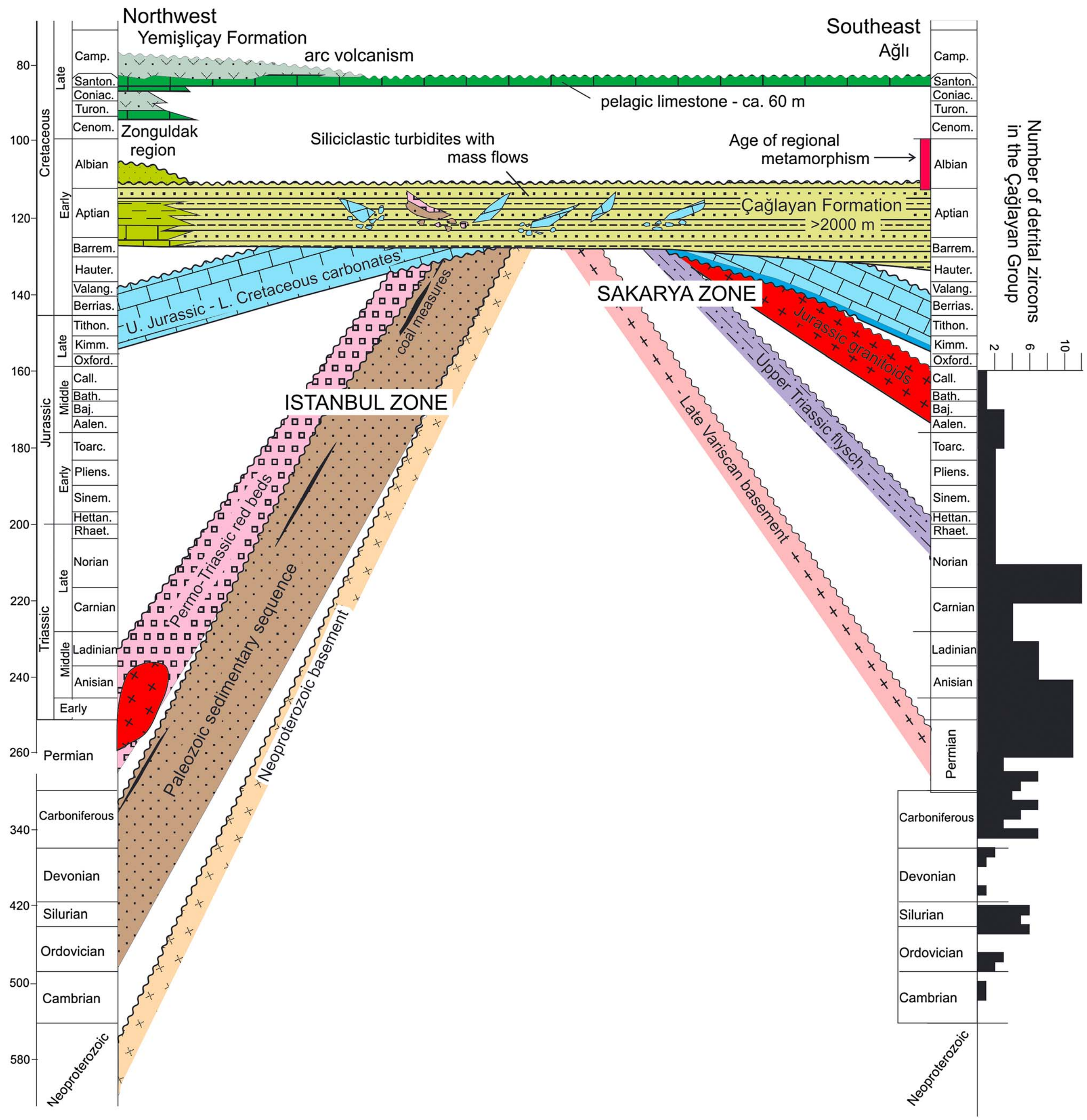

Figure 3. Generalized stratigraphic section of the Central Pontides with emphasis on the Çağlayan Formation. Also shown is the detrital zircon distribution in the sandstones of the Çağlayan Formation.

[14] The turbidites of the Çağlayan Formation are strongly folded and locally faulted. The wavelength and amplitude of folding are generally in meters to tens of meters in scale, and the folds die out both vertically and horizontally over tens to hundred meters distance, which is typical for the deformation of flysch. The attitude of bedding changes over short distances because of folding and slumping. Cleavage is often observed in shales west of Devrekani and is commonly folded, suggesting polyphase deformation. The lack of marker horizons makes the decipherment of the large-scale structures difficult. The age of the deformation is poorly constrained and is usually assumed to be Eocene or younger [*Sunal and Tüysüz*, 2002].

4. The Martin Complex: Metamorphosed Lower Cretaceous Turbidites

[15] In the south, in the region between Devrekani and Araç (Figure 2), the Çağlayan Formation is in contact with a low-grade metamorphic unit, herein called the Martin Complex, which is considered as Triassic or older basement [e.g., *Yılmaz and Şengör*, 1985; *Tüysüz*, 1999; *Ustaömer and Robertson*, 1994, 1999; *Yılmaz et al.*, 1997b; *Yiğitbaş et al.*, 1999; *Uğuz et al.*, 2002]. The Martin Complex is made up predominantly of slate and phyllite with minor intercalated thinly to medium-bedded black recrystallized limestone, metasiltstone, and fine-

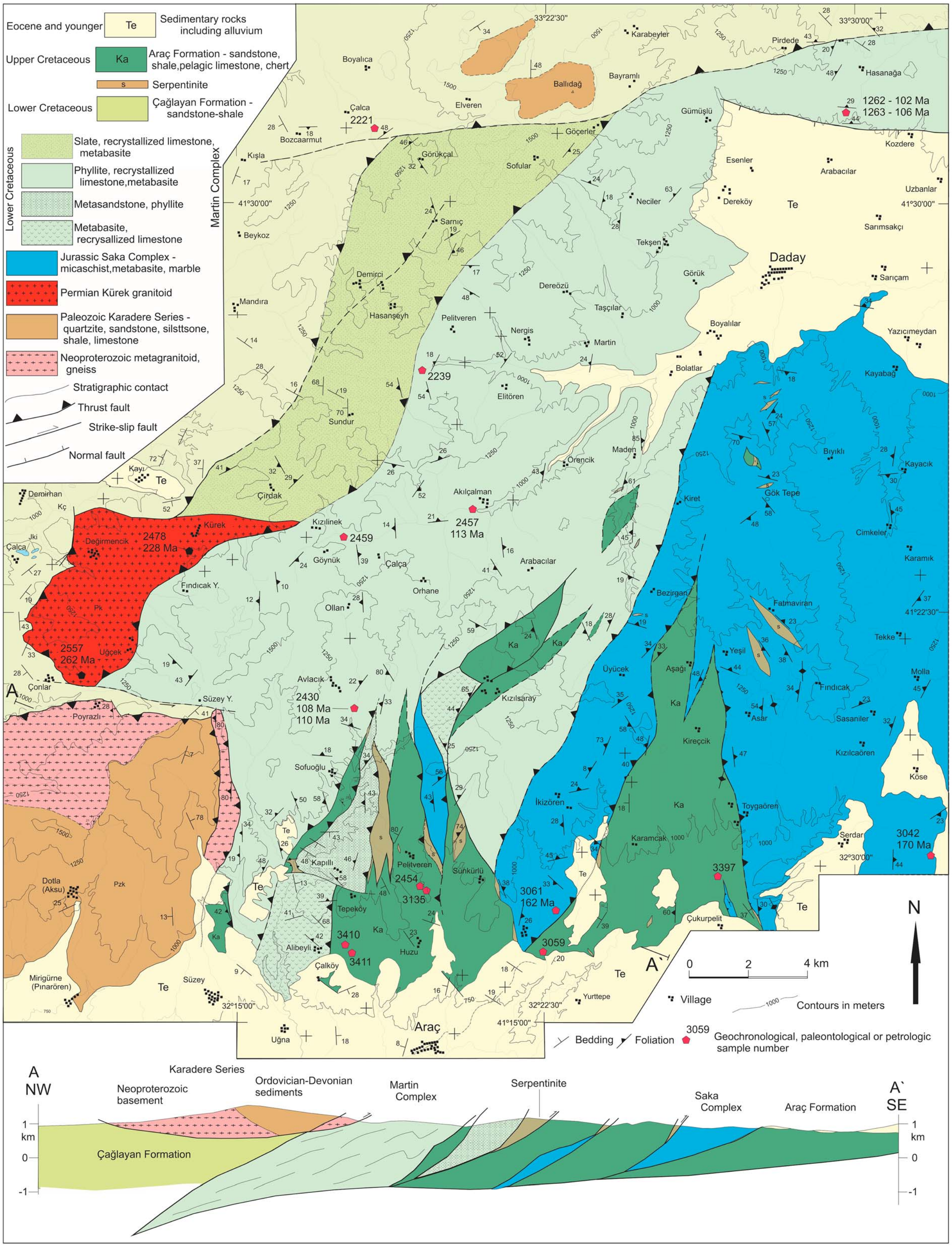

Figure 4. Geological map and cross section of the region between Araç and Daday in the southwestern part of the Central Pontides. For location, see Figure 2.

grained metasandstone. There are also minor (<5%) metabasite and metachert layers within the metaclastics. The metamorphism is in low greenschist facies in regions close to the contact with the Çağlayan Formation, where the dominant rock types are black slates and intercalated thinly bedded recrystallized black limestones. Further southeast, the rocks consist predominantly of phyllites (>80%) with minor marble and metabasite. The metabasites

Table 1. Ar-Ar Age Results

Sample	UTM Coordinates	Formation	Rock Type	Dated Mineral	WTD Mean Age	Error ±	MSWD	No. of Analysis
1262	36 T05 41 483–45 97 700	Martin Complex	Phyllite	Muscovite	102.1	1.0	13.0	15 grains
1263	36 T05 41 513–45 97 409	Martin Complex	Phyllite	Muscovite	105.6	1.3	28.0	18 grains
2430A	36 T05 24 926–45 77 225	Martin Complex	Phyllite	Muscovite in Slab	107.8	1.6	65.0	8 spots
2430B	36 T05 24 926–45 77 225	Martin Complex	Phyllite	Muscovite	110.0	1.6	7.6	10 grains
2430B	36 T05 24 926–45 77 225	Martin Complex	Phyllite	Muscovite in Slab	105.8	2.0	55.0	10 spots
2457	36 T05 28 858–45 84 026	Martin Complex	Phyllite	Muscovite	112.8	1.5	3.1	9 grains
3144	36 T06 38 691–45 69 805	Domuzdağ Complex	Micaschist	Muscovite	114.1	3.3	24.0	13 grains
3148	36 T06 61 656–45 72 910	Domuzdağ Complex	Micaschist	Muscovite	107.0	4.6	3.0	13 grains
2756	36 T05 96 857–46 09 184	Çangaldağ Complex	Phyllite	Muscovite	125.0	1.4	3.0	14 grains
2777	36 T05 96 857–46 09 184	Çangaldağ Complex	Phyllite	Muscovite	136.1	3.8	25.0	15 grains
2912	36 T05 48 516–45 79 051	Saka Complex	Micaschist	Muscovite	163.8	1.5	7.2	10 grains
3042	36 T05 44 386–45 72 326	Saka Complex	Micaschist	Muscovite	170.0	2.4	19.0	9 grains
3061C	36 T05 31 822–45 70 356	Saka Complex	Micaschist	Muscovite	161.5	0.6	0.9	9 grains
3140	36 T06 30 690–45 59 513	Saka Complex	Micaschist	Muscovite	162.2	4.1	6.2	10 grains
2478	36 T05 19 320–45 82 570	Kürek Granitoid	Diorite	Hornblende	228.0	11.0	23.0	10 grains

The UTM coordinates are in the European 1979 grid, which is closely compatible with the 1:25,000 scale topographic maps of Turkey. For full analytical data, see Table 1 in the supporting information.

show a typical greenschist-facies mineral assemblage of actinolite + chlorite + albite + epidote + titanite.

[16] Our geological field mapping of the contact between the Çağlayan Formation and the metamorphic rocks showed that the region consists of a number of north to northwest dipping thrust slices of fine-grained clastic and metaclastic rocks, which show an increasing degree of metamorphism toward the southeast (Figure 4). The thrust slices range from unmetamorphosed distal turbidites of the Çağlayan Formation in the north through slates to phyllites in the southeast. The phyllites are cut by a large number of shear planes, separated by hundreds of meters, suggesting that the Martin Complex constitutes a thrust stack rather than a continuous stratigraphic sequence. Tectonic repetition of metabasite-metachert-phyllite sequences north of Daday supports this inference.

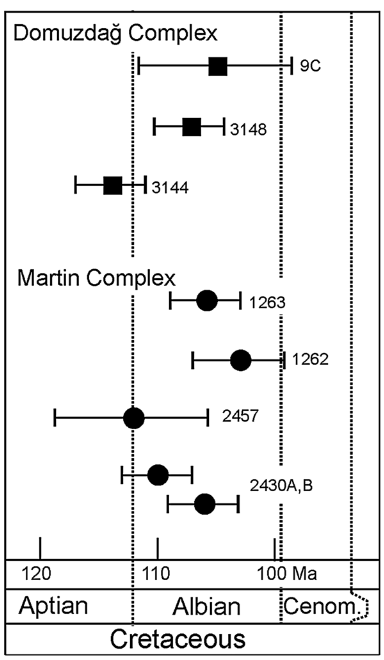

Figure 5. Ar-Ar white mica ages from the Martin and Domuzdağ complexes. For analytical data, see the supporting information. The Ar-Ar age from sample 9C is from *Okay et al.* [2006], and the rest is from this study. Error bars are 2σ.

4.1. Metamorphic Age of the Martin Complex

[17] So far, there have been no age constraints on the Martin Complex apart from the unconformably overlying Lower Eocene limestones. To constrain its age of metamorphism, we have dated muscovites from five phyllite samples using the Ar/Ar laserprobe technique. The samples consist of fine-grained quartz, chlorite, and muscovite (see ds04 in the supporting information). Two methods were used: laser spot dating on polished slabs and single-grain fusion of individual muscovite minerals. The location of the samples is shown in Figure 4, and the Ar/Ar age dating results are summarized in Table 1. Details of mineral separation and dating methods, full Ar/Ar data set, and petrographic description of the dated samples are given in the supporting information. We use *Gradstein et al.* [2004] for the geological timescale.

[18] Muscovite separates from four phyllite samples gave Early Cretaceous (Albian) ages ranging from 102 to 112 Ma (Figure 5); laser spot Ar/Ar ages from the polished slabs for two samples (2430B and 2457) also produced Albian ages similar to those from the muscovite separates (Table 1). The metamorphism is in low greenschist facies, and the metamorphic temperatures were less than 400°C [e.g., *Yardley*, 1989], indicating that the Ar-Ar data represent the age of metamorphism. The age results indicate that the metamorphism of the Martin Complex occurred in the Albian (107 ± 4 Ma) and was coeval or slightly postdated the deposition of the Çağlayan Formation (Figure 3).

4.2. Thrust Sheets Over the Martin Complex

[19] The Çağlayan Formation and the Martin Complex are tectonically overlain by the crystalline basement and the Paleozoic sedimentary sequence of the Istanbul Zone, known as the Karadere Series, and by the Kürek granitoid (Figures 2 and 4). The basement rocks of the Istanbul Zone consist of gneiss and late Neoproterozoic metagranitoid with 590–560 Ma zircon Pb-Pb ages [*Chen et al.*, 2002], which are unconformably overlain by an Ordovician to Devonian sedimentary series [*Boztuğ*, 1992; *Dean et al.*, 2000]. The Rb-Sr biotite ages from the metagranitoid are also Neoproterozoic (548–545 Ma) and show that the Karadere Series were not reset by a subsequent Phanerozoic metamorphic event. In the north, the Karadere Series lie with a low to

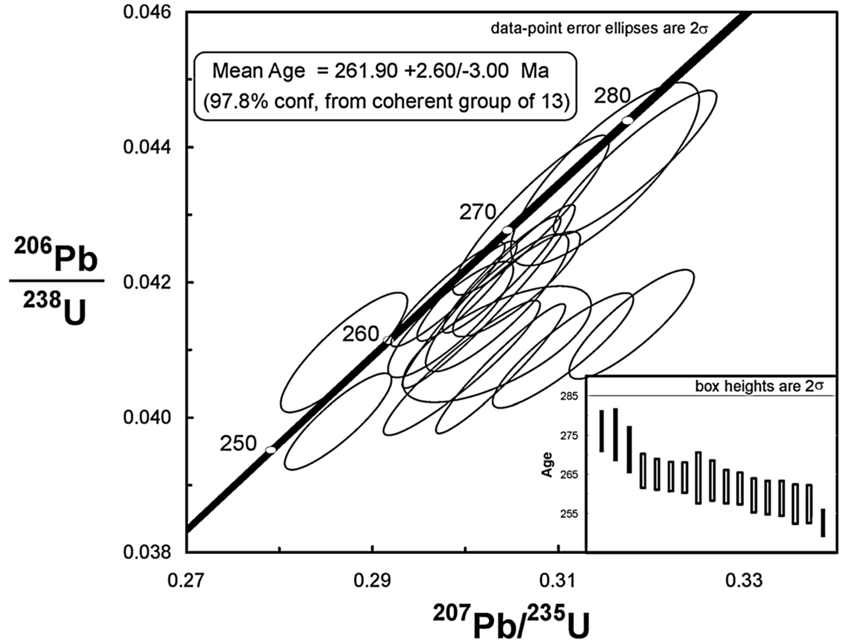

Figure 6. Zircon U-Pb diagram from the Kürek granitoid. For analytical data, see Table 2.

medium dipping tectonic contact over the Çağlayan Formation [*Boztuğ*, 1992, and our observations], and in the east, it lies through an imbricate tectonic zone made up of basement slices over the slates and phyllites of the Martin Complex [Figure 4; *Yiğitbaş et al.*, 1999]. In the structurally upper parts of the Martin Complex close to the overlying thrust sheets, there are blocks, up to 100 m across, of granitoid and quartz-porphyry within the phyllites. Zircons from one granitoid sample produced late Neoproterozoic ages (sample 2459 in Figure 4, circa 598 Ma; Thomas Zack, personal communication), indicating that they were derived from the basement of the Istanbul Zone.

[20] The Kürek granitoid is a bimodal pluton consisting of diorite intruded by granite-granodiorite and is considered as a Jurassic intrusion in the metamorphic rocks of the Martin Complex [*Yılmaz and Boztuğ*, 1986; *Boztuğ*, 1992; *Yiğitbaş et al.*, 1999]. The diorite is made up essentially of plagioclase and hornblende with minor biotite, and the granite-granodiorite comprises plagioclase, K-feldspar, and biotite. Most of the biotite is chloritized, and hornblende is commonly rimmed and replaced by later lighter green calcic amphibole. Our geological mapping showed that the Kürek granitoid does not intrude the phyllites of the Martin Complex but lies tectonically over them (Figure 4). To establish the age of the Kürek granitoid, we have dated zircons from a granitic sample (sample 2557) and hornblendes from a diorite (sample 2478). The U-Pb zircon dating produced a well-constrained Late Permian (262 ± 3 Ma) intrusion age (Figure 6). The hornblende Ar-Ar single grain fusion ages scatter between 256 Ma and 210 Ma with relatively large errors, probably as a result of the late stage subsolidus recrystallization (Table 2). An average hornblende Ar-Ar age of 228 ± 11 Ma ($n = 10$) suggests cooling of the Kürek granitoid during the Middle Triassic. Thus, the Kürek granitoid is an Upper Permian pluton with Triassic cooling ages. Upper Permian granitoids crop out further west in the Istanbul Zone [*Yılmaz*, 1975; *Ustaömer et al.*, 2005; *Bozkurt et al.*, 2012] and are also described from the Strandja Massif [*Okay et al.*, 2001; *Sunal et al.*, 2006] but are not known from the Sakarya Zone.

[21] At least two periods of shortening are present in the area north of Araç. The first one was during the Albian, when the Martin Formation was deformed and metamorphosed. The second deformation phase postdates the deposition of the Upper Cretaceous Araç Formation (see below), which occurs as tectonic slices in the metamorphic rocks (Figure 4). The latter phase is constrained between Santonian, the youngest age from the Araç Formation, and Early Eocene, which is the age of the shallow-marine limestones that cover the tectonic contacts between the metamorphic rocks and the Araç Formation [Figure 4; *Özcan et al.*, 2007; Özcan, personal communication]. It is difficult to differentiate the structures formed during each of these deformation phases, as they have a similar orientation and were probably part of the same progressive shortening process. The attitude of the thrust planes and the shape of the imbricate duplexes (Figure 4) and minor structures (vergence of mesoscopic folds, shear planes) indicate top-to-east-southeast shortening. The pre-Jurassic terrane boundary between the Istanbul and Sakarya zones in the Central Pontides strikes north-south (Figure 1), which controlled the subsequent structures. Furthermore, based on paleomagnetic measurements, *Meijers et al.* [2010a] infer up to 40° anticlockwise rotation in the western part of the Central Pontides during the latest Cretaceous-Paleocene. Adjusting for this rotation, the shortening during the Cretaceous is top-to-south-southeast.

5. Provenance of the Çağlayan Formation and the Martin Complex: Clastic Zircons From the Sandstones

[22] We have dated 310 clastic zircons from three sandstone samples from the Çağlayan Formation and one metasandstone

Table 2. U-Pb Zircon Data for Kürek Granitoid Sample 2557

			Isotopic Ratios					Apparent Ages (Ma)							
U (ppm)	Th (ppm)	U/Th	$^{207}Pb/^{235}U$	± Error	$^{206}Pb/^{238}U$	± Error	Error Corr.	$^{206}Pb/^{238}U$	± (Ma)	$^{207}Pb/^{235}U$	± (Ma)	$^{206}Pb/^{207}Pb$	± (Ma)	Best Age (Ma)[a]	± (Ma)
1145	782	1.5	0.3039	0.0052	0.04212	0.0007	0.93823	265.9	4.3	269.8	3.9	275.0	4.4	265.9	4.3
985	680	1.4	0.3025	0.0076	0.0418	0.0011	0.96054	264.1	6.5	268.1	5.9	272.4	6.5	264.1	6.5
295	257	1.1	0.315	0.0083	0.0436	0.0011	0.80942	275.1	6.7	278.8	6.6	294.7	8.0	275.1	6.7
633	305	2.1	0.3179	0.0055	0.04139	0.00066	0.85778	261.4	4.1	280.1	4.2	278.0	4.6	261.4	4.1
3590[a]	7410	0.5	0.335	0.011	0.031	0.0013	0.74634	197.0	8.2	292.7	8.6	177.0	10.0	292.7	8.6
2261[a]	4122	0.6	0.4443	0.0085	0.0364	0.0007	0.91617	230.4	4.3	374.4	6.2	169.8	3.2	230.4	4.3
665	372	1.8	0.426	0.012	0.04393	0.00065	0.6847	277.1	4.0	359.5	8.4	342.8	7.2	277.1	4.0
1505	1255	1.2	0.3633	0.0064	0.04264	0.0007	0.89861	269.1	4.3	315.2	4.9	287.5	4.8	269.1	4.3
1764	1386	1.3	0.3038	0.0057	0.04074	0.00078	0.9521	257.4	4.8	269.2	4.5	256.6	4.4	257.4	4.8
983	1006	1.0	0.2981	0.005	0.04183	0.00063	0.92922	264.2	3.9	265.8	4.0	261.7	3.8	264.2	3.9
709	403	1.8	0.2984	0.0055	0.04146	0.0007	0.86101	261.9	4.3	265.0	4.3	257.1	4.3	261.9	4.3
605	319	1.9	0.3071	0.0069	0.043	0.00096	0.91662	271.3	6.0	272.3	5.3	276.0	6.5	271.3	6.0
438	237	1.9	0.3183	0.0072	0.04377	0.00087	0.90856	276.1	5.3	280.3	5.6	275.5	6.0	276.1	5.3
685	461	1.5	0.3501	0.0089	0.04214	0.0008	0.89819	266.1	5.0	305.3	6.6	288.6	6.6	266.1	5.0
329	369	0.9	0.3034	0.0063	0.04171	0.00083	0.867	263.4	5.1	268.8	4.9	257.3	4.8	263.4	5.1
109	81	1.4	0.3034	0.0083	0.0411	0.0007	0.66694	259.6	4.4	268.7	6.5	259.6	4.8	259.6	4.4
830	662	1.3	0.2863	0.0047	0.03996	0.00058	0.86861	252.6	3.6	255.5	3.7	247.0	4.3	252.6	3.6
954	679	1.4	0.3002	0.0044	0.04188	0.0006	0.91106	264.5	3.7	266.4	3.4	260.3	3.4	264.5	3.7
651	421	1.5	0.3055	0.0056	0.04198	0.00063	0.86974	265.0	3.9	271.5	4.4	260.4	4.2	265.0	3.9
345	382	0.9	0.2869	0.0056	0.04098	0.00072	0.85595	258.9	4.5	256.5	4.5	247.6	4.5	258.9	4.5
630	399	1.6	0.3105	0.0062	0.04101	0.00069	0.88965	259.1	4.3	274.4	4.8	254.2	4.0	259.1	4.3
816	702	1.2	0.2996	0.0069	0.04075	0.00081	0.93346	257.4	5.0	265.9	5.4	250.8	5.0	257.4	5.0

[a]Measurements are rejected due to their high U and Th amounts and low U/Th ratios.

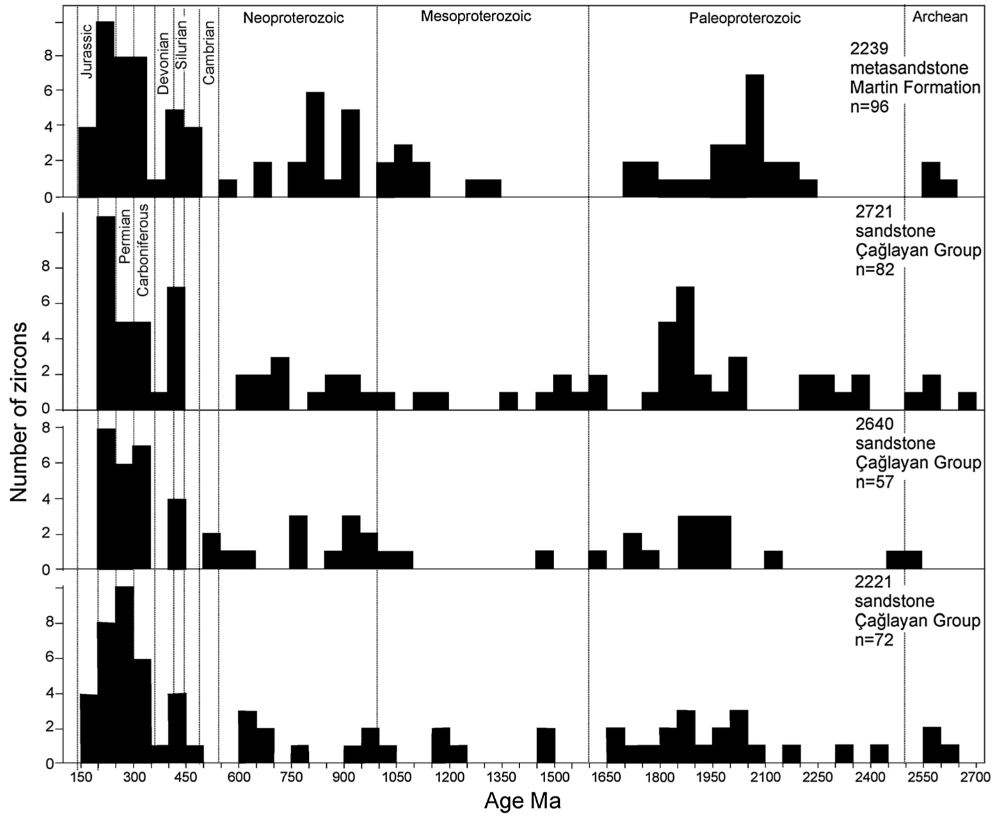

Figure 7. Histograms showing the age distribution of zircons from three sandstone samples from the Çağlayan Formation and one metasandstone from the Martin Complex.

from the Martin Complex to constrain their source and to test their equivalence. The samples come from the southern part of the Çağlayan Formation close to the contact with the Martin Complex (samples 2221, 2239, 2640, and 2721; Figures 2 and 4). Details of the mineral separation, dating method, and the analytical data are given as ds01 and ds03 in the supporting information.

5.1. Depositional age of the Martin Complex

[23] The youngest zircons from the Martin Complex (171 Ma; Figure 7) indicate a post–Early Jurassic depositional age. This, together with its Early Cretaceous (Albian) metamorphic age and the ubiquitous Upper Jurassic-Lower Cretaceous (Kimmeridgian-Berriasian) limestones in the Central Pontides, constrains the deposition of the Martin Complex to Valanginian-Aptian. Lithological similarity between the Martin Complex and the Çağlayan Formation suggests that the Martin Complex has a similar age range (Barremian-Aptian) as the Çağlayan Formation. Furthermore, the clastic zircons from the Çağlayan Formation and the Martin Complex exhibit a similar age pattern (Figures 7 and 9) suggesting a common source. The Early Cretaceous transgression may have started in the south, and the basal age of the Martin Formation can possibly go down to Hauterivian (Figure 12). This is suggested by the Hauterivian nannofossil ages from two samples from the southern part of the Central Pontides in the Ağlı area [*Hippolyte et al.*, 2010]. The clastic zircon ages and the lithological features of the Martin Complex indicate that it represents the metamorphosed distal parts of the Lower Cretaceous turbidites. The metabasite-metachert horizons in the Martin Complex probably represent the upper parts of the oceanic crust on which the turbidites were deposited.

5.2. East European Craton as a Major Source for the Lower Cretaceous Turbidites

[24] The zircon age distribution from the Lower Cretaceous turbidites, including the metasandstone sample from the Martin Complex, shows five prominent peaks (Figure 8): (a) Triassic-Carboniferous, (b) Silurian (432 ± 11 Ma), (c) early Neoproterozoic-Mesoproterozoic, (d) Paleoproterozoic (1800–2100 Ma), and (e) early Paleoproterozoic-late Archean (2400–2550 Ma). Paleoproterozoic zircons are the most common, making up 29% of the total zircon population followed by Paleozoic zircons (26%). Mesozoic and Neoproterozoic zircons each make up 16% of the zircon population trailed by Mesoproterozoic (8%) and Archean (5%) zircons.

[25] No Paleoproterozoic or Archean rocks are known in the Pontides or in Turkey, which has a predominantly late Neoproterozoic basement. An Archean-Paleoproterozoic basement, however, crops out widely in the Ukranian shield and in the East European Craton in general [e.g., *Claesson et al.*, 2006; *Bogdanova et al.*, 2008]. This is well illustrated by the predominantly Paleoproterozoic zircon ages from the present-day sands of the Don and Volga rivers [*Safonova et al.*, 2010; *Wang et al.*, 2011], which drains a major part of the East European Craton (Figure 1). A comparison of the zircon age spectra between those from the Don River

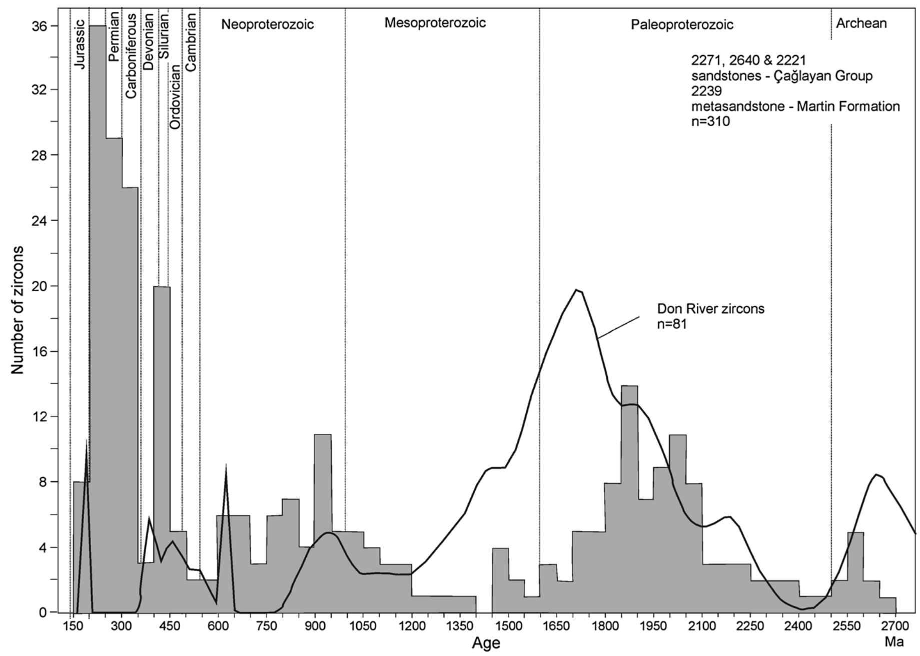

Figure 8. Histogram showing the combined age distribution of zircons from the Lower Cretaceous turbidites (Çağlayan Formation and the Martin Complex). Also shown is the probability density distribution of zircons from the Don River, which drains the Ukranian shield [*Safonova et al.*, 2010].

and those from the Lower Cretaceous turbidites suggests that the early Neoproterozoic-Mesoproterozoic, Paleoproterozoic (1800–2100 Ma), and early Paleoproterozoic-late Archean (2400–2550 Ma) zircons are derived from the East European Craton or from its cover sediments (Figure 8). Another possibility is that the Archean-Paleoproterozoic zircons are second-generation zircons from the Triassic Flysch of the Pontides and Crimea (Figures 2 and 3). However, recent clastic zircon data from the Triassic Flysch show the dominance of Phanerozoic ages with only a few Archean and Paleoproterozoic zircons [*Karslıoğlu et al.*, 2012].

[26] In contrast to the East European Craton, Neoproterozoic granitoids are widespread in the Gondwana-derived terranes, including the Istanbul Zone, which has a basement dominated by late Neoproterozoic granitoids [590–560 Ma; *Chen et al.*, 2002; *Ustaömer et al.*, 2005; *Bozkurt et al.*, 2012]. Late Neoproterozoic clastic zircons (640–520 Ma) also form a dominant population in the Paleozoic sediments of the Istanbul Zone including the Carboniferous and Ordovician sandstones [Figure 9; *Okay et al.*, 2010; *Ustaömer et al.*, 2011]. The sediments in the Lesser Caucasus are also characterized by predominantly late Neoproterozoic zircon populations [Figure 9; *Vincent et al.*, 2013]. Their scarcity in the Çağlayan Formation (Figure 8) indicates that the Istanbul Zone was not an important source for the Lower Cretaceous turbidites.

[27] The Phanerozoic zircons from the Lower Cretaceous turbidites show a broad peak in the Early Jurassic-Carboniferous and a narrow well-defined peak in the Silurian (Figure 10). The Jurassic zircons were most probably derived from the Middle Jurassic granitoids in the northeastern part of the Central Pontides [Figure 2; *Yılmaz and Boztuğ*, 1986]. The

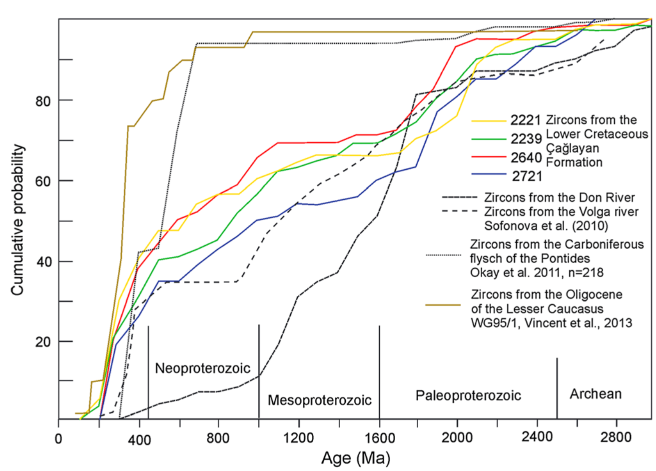

Figure 9. Cumulative probability plot for selected zircon ages from the Black Sea region.

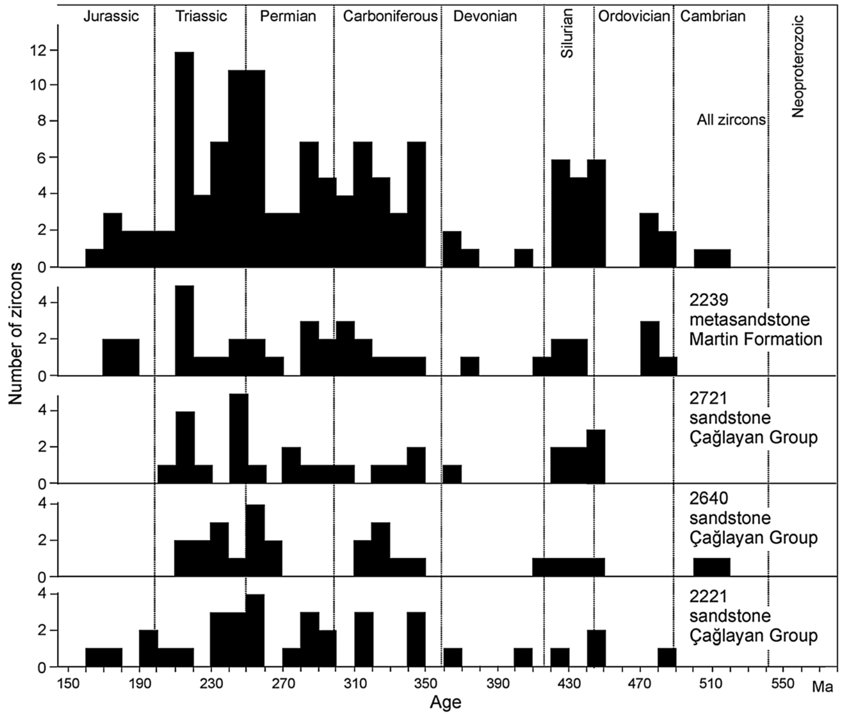

Figure 10. Histogram showing the Phanerozoic zircon ages from three sandstone samples from the Çağlayan Formation and one metasandstone from the Martin Complex.

Permo-Carboniferous zircons may have also a source in the same region [*Nzegge et al.*, 2006]. However, there is no known source for the Triassic and Silurian zircons in the Pontides; they must be derived from the Scythian Platform and the East European Craton (Figure 1). *Alexandre et al.* [2004] describe Triassic and Permian acidic to intermediate volcanic rocks from the Scythian Platform and from the Donbas fold belt; plutonic equivalents may exist under the Neogene cover of the Scythian Platform or in the wide northern submarine shelf of the Black Sea. Orthogneisses with Silurian zircons crop out in the crystalline core of the Greater Caucasus [Main Range Zone, Azau gneisses; *Somin*, 2011, p. 571–573] and may extend north and west toward the Scythian Platform (Figure 1).

[28] Detrital zircons from the Lower Cretaceous turbidites suggest a major source in the East European Craton and possibly in the Scythian Platform with a lesser contribution from the Variscan and Jurassic granitoids of the Sakarya Zone in the Central Pontides. A northerly source is also supported by a southward decrease in the grain size and in the size and density of the blocks in the turbidites.

6. Central Pontide Supercomplex

[29] In the Central Pontides, the Lower Cretaceous turbidites are bounded in the south by a large area of metamorphic rocks, 200 km by 60 km, herein referred to as the Central Pontide Supercomplex (Figure 1), which is considered as Triassic or older basement [e.g., *Yılmaz and Şengör*, 1985; *Tüysüz*, 1999; *Ustaömer and Robertson*, 1994, 1999; *Yılmaz et al.*, 1997b; *Uğuz et al.*, 2002]. The Central Pontide Supercomplex is separated by Tertiary cover into three subareas: the Daday Massif in the west, the Kargı Massif in the east, and the Çangaldağ Complex in the north (Figure 2). We have studied the western part of the Daday Massif in detail and made traverses across the Kargı Massif and the Çangaldağ Complex, and dated some of the samples collected. The petrographic description of the dated samples and the analytical data are given as supporting information. Based on our studies and on earlier work [*Tüysüz and Yiğitbaş*, 1994, *Okay et al.*, 2006; *Yılmaz et al.*, 1997a], three metamorphic belts of (1) Middle Jurassic, (2) Early Cretaceous, and (3) middle Cretaceous ages are distinguished within the Central Pontide Supercomplex (Figure 2).

6.1. Middle Jurassic Saka Complex

[30] The Saka Complex consists mainly of micaschists, which make up about 80% of the metamorphic sequence; the rest is made up of marble, calc-schist, metabasite, and small serpentinite slivers. It crops out mainly in the Daday

Table 3. Modes of the Analyzed Samples From the Saka Complex

	Garnet-Micaschists			Amphibolite
Sample	3061C	3064	3099	3061B
Quartz	31	20	38	8
Plagioclase	19	–	–	31
Garnet	14	28	19	18
Kyanite	–	6	11	–
Hornblende	–	–	–	38
Biotite	4	2	2	–
Muscovite	25	22	20	tr.
Chlorite	3	7	8	1
Epidote	tr.	–	–	3
Rutile	2	2	2	1
Titanite	–	–	–	tr.
Opaque	2	3	1	–
Apatite	tr.	–	–	tr.

tr, less than 0.5%.

Table 4. Representative Mineral Compositions from the Saka Complex[a]

	gtr	gtr	gtr	gtr		plag	plag		hbl		biot		mu	mu	mu		chl	chl	chl
	3061C	3061B	3064	3099		3061C	3061B		3061B		3061C		3061C	3064	3099		3061C	3064	3099
	40	95	23	117		58	114		96		77		49	32	116		43	25	122
SiO_2	37.46	38.00	38.52	38.08		59.65	59.79		43.22		36.18		46.76	46.42	46.74		26.10	26.11	26.15
TiO_2	0.00	0.04	0.06	0.05		0.00	0.04		0.85		1.77		0.93	1.01	1.44		0.06	0.07	0.13
Al_2O_3	21.50	21.62	22.44	21.82		25.33	24.88		15.14		17.02		34.08	33.90	33.27		21.30	22.86	22.16
Cr_2O_3	0.03	0.06	0.00	0.05		0.01	0.00		0.02		0.07		0.06	0.08	0.04		0.01	0.09	0.05
FeO	30.95	25.23	28.01	30.96		0.05	0.02		14.35		14.67		1.06	1.47	1.30		22.13	17.91	21.95
MnO	1.15	0.84	1.76	2.04		0.00	0.02		0.01		0.19		0.00	0.04	0.00		0.23	0.13	0.57
MgO	6.12	3.31	6.24	6.53		0.00	0.01		10.53		13.89		1.51	1.64	1.70		18.20	20.48	18.28
CaO	3.49	11.65	5.03	2.12		6.65	6.33		11.58		0.21		0.02	0.00	0.00		0.05	0.02	0.00
Na_2O	0.03	0.01	0.03	0.03		8.47	8.44		1.92		0.06		1.45	1.11	1.33		0.04	0.00	0.00
K_2O	0.03	0.01	0.02	0.01		0.09	0.10		0.75		6.88		9.32	9.60	9.50		0.02	0.00	0.01
F	0.00	0.00	0.04	0.03		0.00	0.00		0.00		0.36		0.11	0.00	0.09		0.07	0.00	0.00
Total	100.77	100.78	102.14	101.71		100.26	99.64		98.38		91.29		95.30	95.27	95.40		88.21	87.67	89.29
Si	2.947	2.971	2.960	2.963		2.679	2.698		6.283		2.784		3.108	3.093	3.112		2.690	2.640	2.658
Ti	0.000	0.002	0.004	0.003		0.000	0.001		0.093		0.102		0.046	0.051	0.072		0.004	0.006	0.010
Al	1.993	1.992	2.032	2.002		1.341	1.323		2.594		1.544		2.670	2.662	2.610		2.587	2.724	2.654
Cr	0.002	0.004	0.000	0.003		0.000	0.000		0.002		0.004		0.003	0.004	0.002		0.001	0.007	0.004
Fe^{3+}	0.058	0.030	0.004	0.029					0.425										
Fe^{2+}	1.977	1.620	1.795	1.985		0.002	0.001		1.320		0.944		0.059	0.082	0.072		1.907	1.514	1.866
Mn	0.062	0.045	0.094	0.109		0.000	0.001		0.001		0.010		0.000	0.002	0.000		0.016	0.009	0.040
Mg	0.718	0.386	0.715	0.758		0.000	0.001		2.282		1.593		0.149	0.163	0.168		2.796	3.087	2.770
Ca	0.294	0.976	0.414	0.177		0.320	0.306		1.821		0.017		0.002	0.000	0.000		0.005	0.002	0.000
Na	0.004	0.002	0.004	0.003		0.612	0.613		0.454		0.008		0.155	0.119	0.142		0.007	0.000	0.000
K	0.003	0.001	0.002	0.001		0.005	0.006		0.141		0.675		0.790	0.816	0.807		0.002	0.000	0.002
	8.059	8.029	8.023	8.034		4.959	4.949		15.417		7.681		6.982	6.991	6.985		10.016	9.989	10.004
alm	0.20	0.12	0.16	0.23	an	0.46	0.44	tr	0.0761	phl	0.097	mu	0.59	0.60	0.56	clin	0.058	0.103	0.057
gr	0.0020	0.0460	0.0060	0.00050	ab	0.70	0.71	fact	0.00075	ann	0.0112	cel	0.056	0.042	0.060	daph	0.0081	0.0033	0.0083
py	0.023	0.009	0.026	0.024				parg	0.016	east	0.075	fcel	0.021	0.021	0.026	ames	0.055	0.091	0.056
												pa	0.71	0.52	0.67				

[a]Activities are calculated at 620° C and 10 kbar. Abbreviations: ab, albite; alm, almandine, an, anorthite; ann, annite; ames, amesite; cel, celadonite; clin, clinochlore; daph, daphnite; east, eastonite; fact, Fe-actinolite; fcel, Fe-celadonite; gr, grossular; mu, muscovite; pa, paragonite; parg, pargasite; phl, phlogopite; py, pyrope; tr, tremolite.

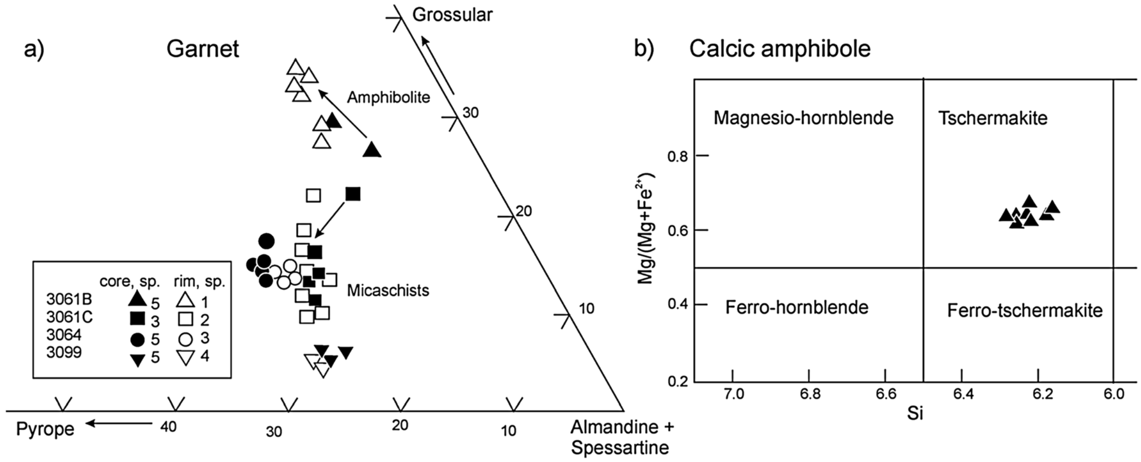

Figure 11. Garnet and amphibole compositions from the metamorphic rocks of the Saka Complex. Arrows indicate core to rim zoning.

Massif lying tectonically below the Martin Complex. Slices of the Saka Complex are also tectonically imbricated with the Martin Complex (Figure 4). A similar metamorphic sequence dominated by micaschists crops out in the southern part of the Kargı Massif [Figure 2; *Tüysüz and Yiğitbaş*, 1994].

6.1.1. Petrology and Thermobarometry

[31] The prevalent mineral paragenesis in the micaschists of the Saka Complex in the Daday Massif is quartz + plagioclase + muscovite + chlorite ± garnet ± biotite ± kyanite, and that in the metabasites is actinolite/hornblende + plagioclase + chlorite + epidote/clinozoisite ± garnet. In the micaschists, garnet forms porphyroblasts with quartz and white mica inclusions. Biotite is less common than garnet, and when found, it occurs in amounts of less than five modal percent. Kyanite forms porphyroblasts, which are partially replaced by very fine grained white mica aggregates. To constrain the pressure-temperature (P-T) conditions of metamorphism, minerals from three micaschists and one garnet-amphibolite were analyzed by electron microprobe. The estimated mineral modes of these samples are given in Table 3 and representative mineral compositions in Table 4. Analyzed garnets are almandine-pyrope-grossular solid solutions with less than 5 mol % spessartine end member (Figure 11a and Table 3). They show minor growth zoning not exceeding a few mole percent. Muscovite is characterized by Si cation values of 3.04–3.15 in the 11 oxygen formula unit. Plagioclase compositions range from albite to andesine even in a single sample because of the late stage alteration. Biotites show deficiencies in the alkali sites. Calcic amphiboles from the garnet-amphibolite are tschermakites (Figure 11b).

[32] The P-T conditions were estimated from the analyzed mineral assemblages using the THERMOCALC program of *Powell and Holland* [1988] with the thermodynamic data set of *Holland and Powell* [1998]. The mineral activities were determined using the AX program (http://www.esc.cam.ac.uk/research/research-groups/holland/ax) from the representative mineral compositions listed in Table 4. Mineral equilibria constrain the temperatures of metamorphism fairly precisely at 620°C, and pressures are less well constrained to between 8 and 12 kbar (Figure 12). The P-T conditions of metamorphism of 620 ± 30°C and 10 ± 2 kbar correspond to high-pressure amphibolite facies.

6.1.2. Geochronology

[33] Muscovite separates from the Saka Complex—three micaschists from the Daday Massif and one from the Kargı Massif—were dated using single-grain Ar-Ar method to constrain the age of metamorphism. The muscovite Ar-Ar ages are Middle Jurassic ranging between 162 and 170 Ma (Figure 13 and Table 1). Considering the estimated temperature of metamorphism of 620 ± 30°C and the closure temperatures for the Ar-Ar system in muscovite, the Middle Jurassic ages represent cooling ages.

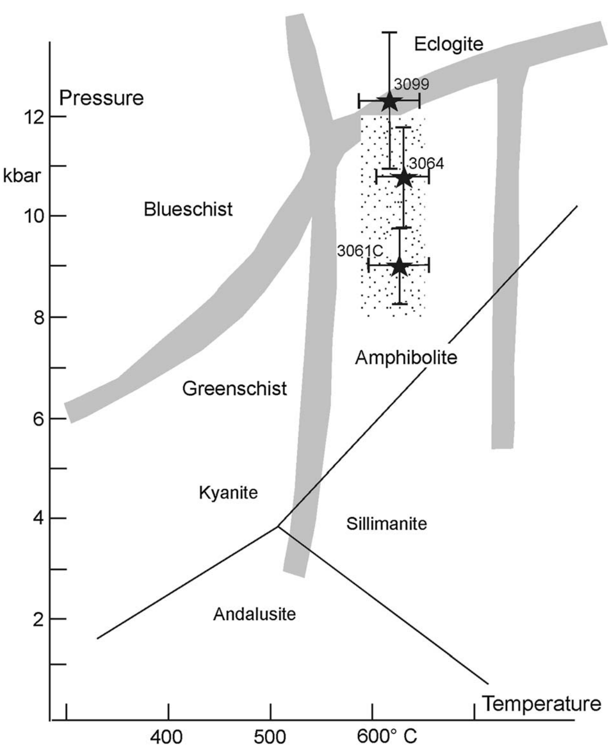

Figure 12. Pressure-temperature diagram showing the estimated conditions of metamorphism of the Saka Complex. The facies fields are after *Yardley* [1989] and *Evans* [1990]. The reactions shown are calculated by THERMOCALC using the activities in Table 3.

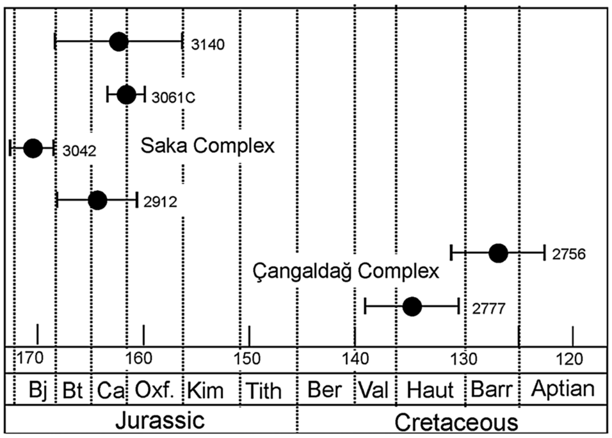

Figure 13. Ar-Ar white mica ages from the Saka and Çangaldağ complexes. For analytical data, see the supporting information. Error bars are 2σ.

[34] Lower-Middle Jurassic metamorphic rocks, lithologically similar to those from the Saka Complex, have been recently described from the İzmir-Ankara suture zone in the Çankırı [*Çelik et al.*, 2011] and Erzincan areas [*Topuz et al.*, 2013] and have been interpreted as a Jurassic subduction-accretion complex. In view of its tectonic setting and the relatively high pressures during its metamorphism, the Saka Complex probably constitutes part of the same accretionary complex.

6.2. Çangaldağ Complex: Early Cretaceous Metamorphism

[35] The Çangaldağ Complex is an over 10 km thick tectonic stack of volcanic, volcaniclastic, and fine-grained clastic rocks metamorphosed in low greenschist facies, which is interpreted either as an ophiolite [*Yılmaz*, 1980, 1988; *Tüysüz*, 1990] or as an ensimatic volcanic arc [*Ustaömer and Robertson*, 1993]. The geochemistry of the volcanic rocks suggests the latter alternative [*Ustaömer and Robertson*, 1999]. The volcanic rocks are mainly andesite with lesser amounts of basaltic andesite and dacite.

[36] The fine-grained clastic rocks, which make up about 20% of the Çangaldağ sequence, are represented by phyllites consisting of quartz, white mica, and chlorite. The fine-grained volcanic rocks have recrystallized to albite + chlorite + actinolite + epidote assemblages. In the more massive volcanic and subvolcanic rocks, the volcanic textures and augite have survived the metamorphism. We have dated white micas from two phyllites (samples 2756 and 2777) from the Çangaldağ Complex (Figure 2). The Ar-Ar single-grain ages are 125 ± 1 Ma and 136 ± 4 Ma and indicate an Early Cretaceous (Valanginian-Barremian) age for the regional metamorphism (Figure 13 and Table 1).

6.3. Middle Cretaceous Metamorphic Belts

[37] Most of the Central Pontide Supercomplex consists of middle Cretaceous (Albian) metamorphic rocks. These include the Martin Complex, described above, and the Domuzdağ and Esenler complexes, which make up the bulk of the Kargı Massif (Figure 2). The Domuzdağ Complex forms a broad belt of eclogite and high-grade blueschist variously overprinted by greenschist-facies metamorphism. Ar-Ar and Rb-Sr isotopic data from the Domuzdağ Complex indicate a middle Cretaceous age (circa 105 Ma) for the metamorphism [*Okay et al.*, 2006] same as that of the Martin Complex (Figure 5). The eclogite-facies and blueschist-facies rocks pass southward to a large metamorphic area made up mainly of metabasite with minor micaschist and marble apparently with only greenschist-facies mineral assemblages (Figure 2). We have dated white micas from two micaschists (samples 3144 and 3148) from this region to constrain the age of the metamorphism. The Ar-Ar ages are middle Cretaceous (114 Ma and 107 Ma; Figure 2 and Table 1) similar to those from the Domuzdağ Complex. We interpret this metamorphic region as the southward continuation of the Domuzdağ Complex, where the high-pressure mineral paragenesis has been obliterated.

[38] The Domuzdağ Complex is tectonically overlain in the north by a low-grade blueschist belt of phyllite and metasandstone with minor metabasite and marble, called the Esenler Complex. The Esenler Complex differs from the Domuzdağ Complex by being a dominantly metasedimentary unit with the metabasites making up less than 5% of the sequence, and it shows a low-grade blueschist-facies metamorphism. Sodic amphibole occurs widely in the metabasic rocks of the Esenler Complex. The Esenler Complex extends westward to south of Kastamonu, where rare metabasite horizons contain the mineral assemblage sodic amphibole + epidote + albite + chlorite + titanite. The K-Ar data from the Esenler Complex by *Yılmaz et al.* [1997a], although widely scattered, indicate a broad middle Cretaceous age for its metamorphism.

6.4. Tectonic Architecture of the Central Pontide Supercomplex

[39] The Central Pontide Supercomplex (CPS) is made up of ENE trending metamorphic belts of Middle Jurassic (170–160 Ma), Early Cretaceous (135–125 Ma), and middle Cretaceous (107 ± 4 Ma) ages (Figure 2). The lithological features and the metamorphic facies suggest that these metamorphic belts represent distinct subduction-accretion units of the Tethys. In a progressive subduction-accretion model, the ages of the accreted sequences are expected to young toward the active subduction zone. However, such an arrangement is not observed in the Central Pontide Supercomplex, where there is a repetition of the middle Cretaceous and Middle Jurassic metamorphic belts. This could be due to out-of-sequence thrusting, strike-slip emplacement, or subsequent deformation.

7. Upper Cretaceous Sequences

7.1. Upper Cretaceous Pelagic Carbonates and Volcanic Rocks

[40] In the Central Pontides, the Çağlayan Formation is unconformably overlain by Upper Cretaceous red pelagic limestones (Figure 2), which also crop out widely in the Eastern Pontides, where they rest on rocks as old as Carboniferous granitoids [*Görür et al.*, 1993; *Okay and Şahintürk*, 1997]. They represent rapid subsidence of the Central and Eastern Pontides following a period of subaerial erosion. Their deposition is generally related to the rift-drift transition and the start of oceanic spreading in the Black Sea back-arc basin and the ensuing thermal subsidence [*Görür*, 1988, 1997; *Hippolyte et al.*, 2010; *Tüysüz et al.*, 2012].

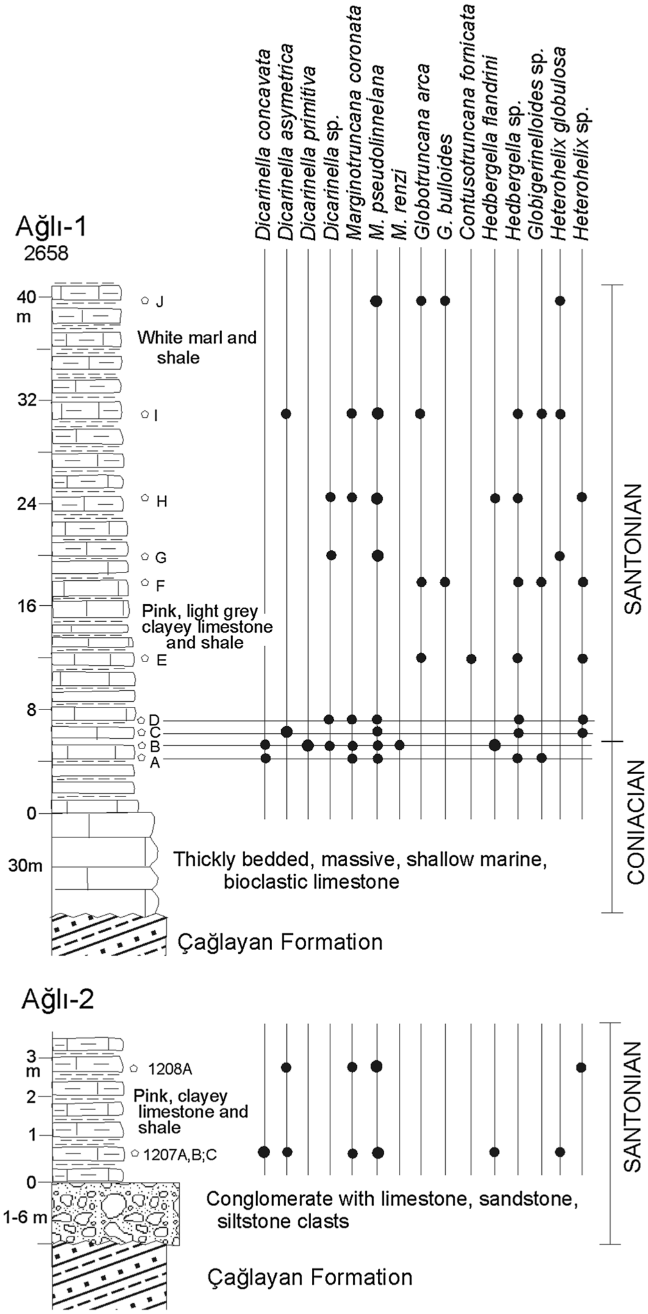

Figure 14. Measured stratigraphic sections in the Upper Cretaceous pelagic limestones. For location of the sections, see Figure 2.

[41] In the north, within 15 km of the Black Sea margin, the deposition of the red pelagic limestones starts at late Cenomanian-Turonian, and they are locally intercalated with volcanic rocks, which mark the inception of arc magmatism in the Pontides [*Yılmaz et al.*, 2010; *Tüysüz et al.*, 2012]. Further south, the red pelagic limestones lie unconformably over the Çağlayan Formation but with no associated Cretaceous volcanism. To constrain this first marine transgression over the Çağlayan Formation, two sections in the pelagic limestones were measured and sampled in the Ağlı region (Figure 2). In the Ağlı-1 section, the turbidites of the Çağlayan Formation are unconformably overlain by a 30 m thick, thickly bedded to massive, white, shallow marine carbonate, which yielded no age-diagnostic fossils. Thinly bedded pink limestones and intercalated thin red shales lie sharply over the shallow marine carbonates and pass up into white marl (Figure 14). The base of the section is Coniacian in age as indicated by the coexistence of *Marginotruncana renzi* and *Dicarinella concavata* (Figure 15). The rest of the 46 m thick section contains middle to upper Santonian fauna (Figures 14 and 15). In the Ağlı-2 section (1207), the black shales of the Çağlayan Formation are overlain by a 3 m thick basal conglomerate with limestone, sandstone, and siltstone clasts, 0.5 cm to 15 cm across (Figure 14). Thinly bedded red to pale pink pelagic limestones with thin shale interbeds lie over the conglomerate and pass up gradually to white marl and shale. Samples close to the base of the Ağlı-2 section contain *Dicarinella asymetrica*, a zone fossil for the Santonian (Figure 15). In both the Ağlı-1 and Ağlı-2 sections, the pelagic carbonates are overlain by Upper Campanian-Maastrichtian marine sandstone, sandy limestone, and sandy marl [*Kennedy et al.*, 2007].

[42] The Hanönü area, 80 km east of the Ağlı region, also exposes the extreme southeastern outcrops of the Çağlayan Formation and the overlying red pelagic limestones (Figure 2). Several sections measured in the red pelagic limestones in this area produced Santonian ages [*Okay et al.*, 2006]. However, as different from the Ağlı region, the red pelagic limestone in the Hanönü area pass up and are intercalated with Santonian volcanic rocks. They are unconformably overlain by the late Campanian-Maastrichtian turbidites.

[43] The period of uplift and erosion of the Çağlayan Formation in the central part of the Central Pontides is constrained between Albian and Turonian. The window of uplift narrows northward, where within a 15 km wide coastal zone, the base of the red pelagic limestones is late Cenomanian [*Yılmaz et al.*, 2010]. In the coastal regions, the pelagic limestone deposition is also accompanied by submarine volcanism, which is markedly absent further south. Based on the distribution of the Upper Cretaceous volcanic and subvolcanic rocks, a volcanic front can be delineated in the Central Pontides (Figure 2). The volcanic front makes a broad arch mimicking the present coastline of the Black Sea and is also subparallel to the trend of the major structures in the area (Figure 2). Based on paleomagnetic data, *Meijers et al.* [2010a] date the formation of this arc-like curvature in the Central Pontides to the latest Cretaceous-Paleocene interval.

7.2. Upper Cretaceous Pelagic Carbonates and Clastic and Volcanic Rocks: The Araç Formation

[44] The Upper Cretaceous pelagic limestone sequence does not extend south to the Central Pontide Supercomplex, where the age equivalent strata consist of a volcano-sedimentary series. In the Daday Massif, this Araç Formation consists of, in order of decreasing abundance, volcanogenic sandstone and shale, thinly bedded red pelagic limestone, dark gray graywacke-siltstone-shale, basaltic pillow lava, red and green radiolarian chert, calciturbidite, mass flows, and serpentinite. The mass flows consist mainly of debris flows, up to 5 m thick, interbedded with pelagic limestone and calciturbidites; the clasts in the debris flows are mainly basalt and limestone. Calciturbidites contain Orbitolinid grains derived from an Aptian-Cenomanian carbonate bank.

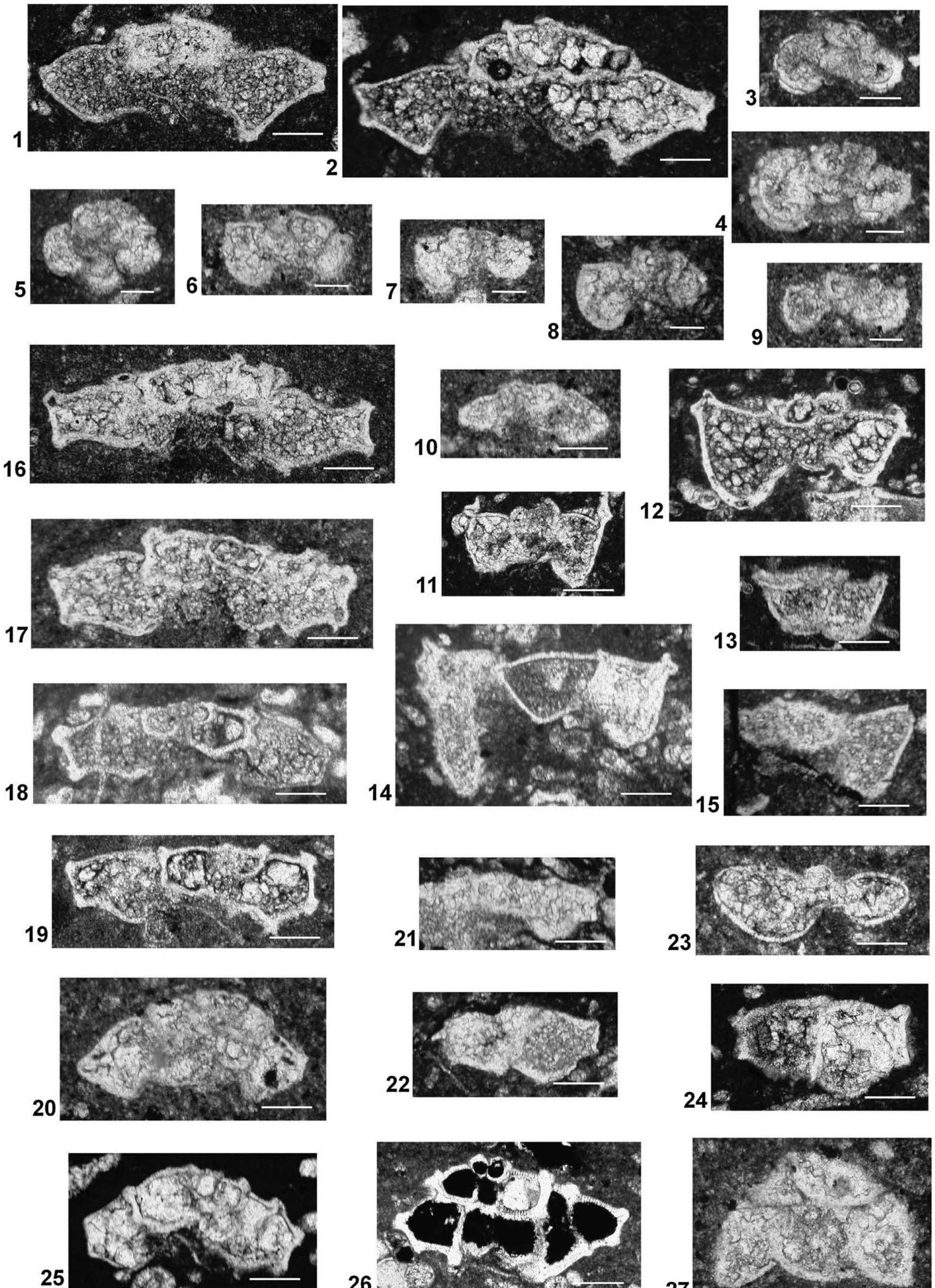

Figure 15. Thin section photomicrographs of some important microfossils from the Upper Cretaceous pelagic limestones (samples 1207, 2658, and 3617) and from the Araç formation (samples 2454, 3397, 3410, and 2411). Scale bar is 0.1 mm. (1 and 2) *Marginotruncana renzi* (Gandolfi, 1942) 2658B. (3 and 4) *Whiteinella praehelvetica* (Trujillo, 1960) 3397C. (5) *Whiteinella paradubia* (Sigal, 1952) 3397C. (6–9) *Helvetoglobotruncana helvetica* (Bolli, 1945) 3410. (10) *Dicarinella algeriana* (Caron, 1966) 3410. (11, 14, and 15) *Dicarinella asymetrica* (Sigal, 1952) (11) 2658I, (14) 3617B, and (15) 2454E. (12 and 13) *Dicarinella concavata* (Brotzen, 1934) (12) 3617B and (13) 2658A. (16) *Marginotruncana coronata* (Bolli, 1945) 2658B. (17–19) *Marginotruncana pseudolinneiana* (Pessagno, 1967) (17) 2658A, (18) 3617B, and (19) 2658B. (20) *Marginotruncana schneegansi* (Sigal, 1952) 3410. (21 and 22) *Dicarinella primitiva* (Dalbiez, 1955) 3411. (23) *Hedbergella flandrini* (Porthault, 1970) 1207A. (24) *Globotruncana bulloides* (Vogler, 1941) 2658F. (25 and 26) *Globotruncana arca* (Cushman, 1926) (25) 2658E and (26) 2658I. (27) *Praeglobotruncana gibba* (Klaus, 1960) 3410.

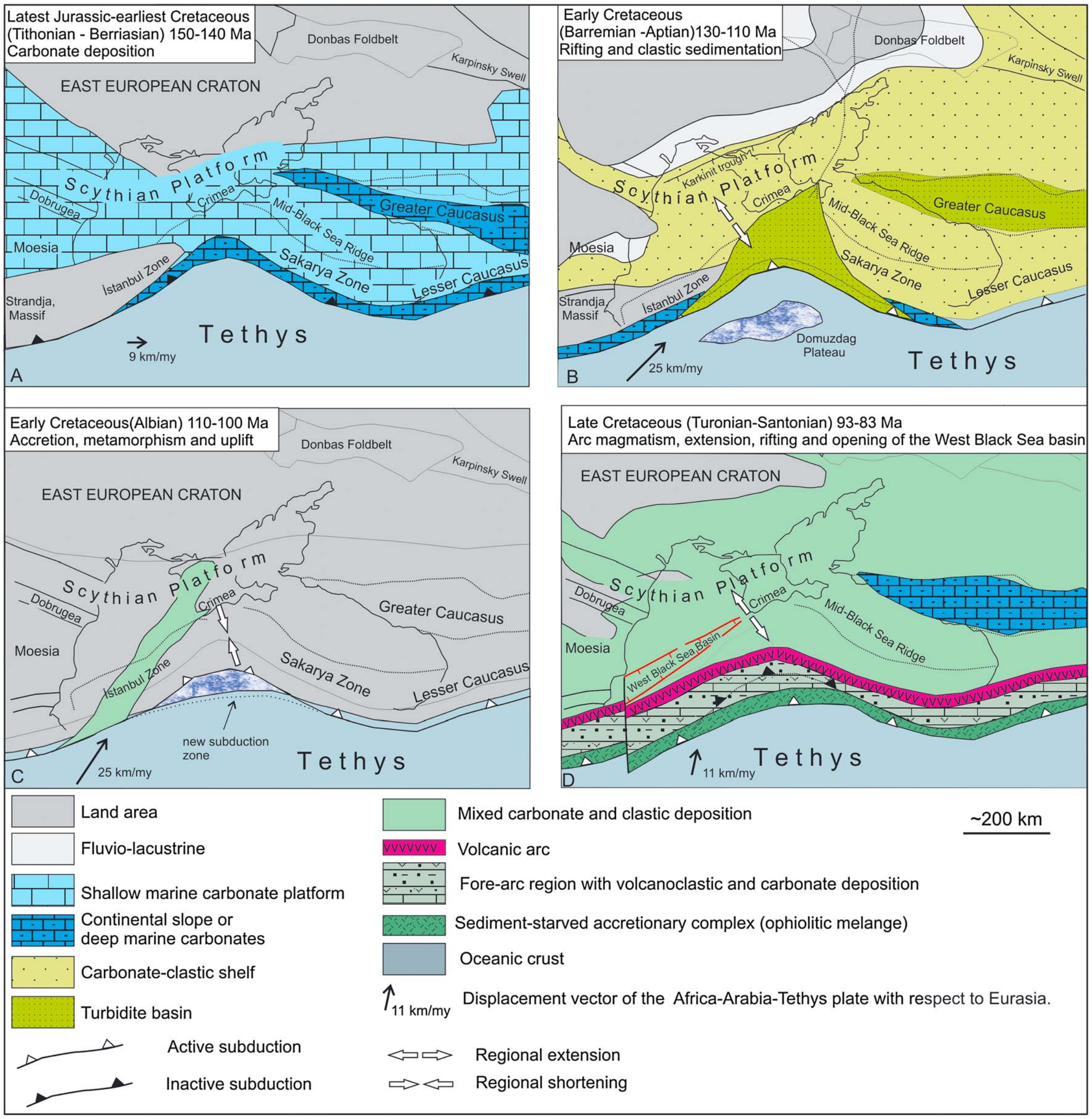

Figure 16. Paleogeographic maps for the southern Pontide-Caucasus margin of the Eurasia for the Late Jurassic-Cretaceous. The maps are based on *Tüysüz* [1999], *Barrier and Vrielynck* [2008], *Adamia et al.* [2011], *Nikishin et al.* [2012], and this study. The plate velocities are estimates from *Smith* [2006] for a location in the Eastern Pontides.

[45] The Araç Formation is tectonically imbricated with the metamorphic rocks; serpentinite slices commonly mark the contacts (Figure 4). In general, the Araç Formation is not metamorphosed; however, some of the thinner slices show development of foliation. The Araç Formation ranges from a coherent sequence, which makes up about 80% of the unit, to a broken formation or mélange. The mélange type deformation is especially observed in the dark graywacke-siltstone-shale horizons.

[46] The Araç Formation is unconformably overlain by Lower Eocene shallow-marine limestone and marl [*Özcan et al.*, 2007], which also cover the tectonic contacts in the metamorphic rocks. Paleontological study of over 30 samples from the pelagic limestones of the Araç Formation showed that its age ranges from Turonian to Santonian. A Turonian age is indicated by the pelagic foraminifera of *Helvetoglobotruncana helvetica*, *Whiteinella pradubia*, *W. praehelvetica*, *Hedbergella planispira*, *Dicarinella algeriana*, *Marginotruncana sigali*, and *Praeglobotruncana gibba* (samples 2889, 3059, 3397, and 3410; Figures 4 and 15). *Marginotruncana pseudolinneiana*, *M. marginata*, *M. renzi*, *and Dicarinella primitive* in sample 3411 give an uppermost Turonian to Coniacian age. The following fauna from samples 2454 and 3135 indicate a Santonian age: *Dicarinella asymetrica*, *Hedbergella flandrini*, *Marginotruncana coronata*, and *M. pseudolinneiana* (Figure 15).

[47] The stratigraphic base of the Araç Formation is not observed; however, debris flows contain abundant clasts of phyllite and micaschist, which suggests that the Araç Formation might have been deposited partly on the

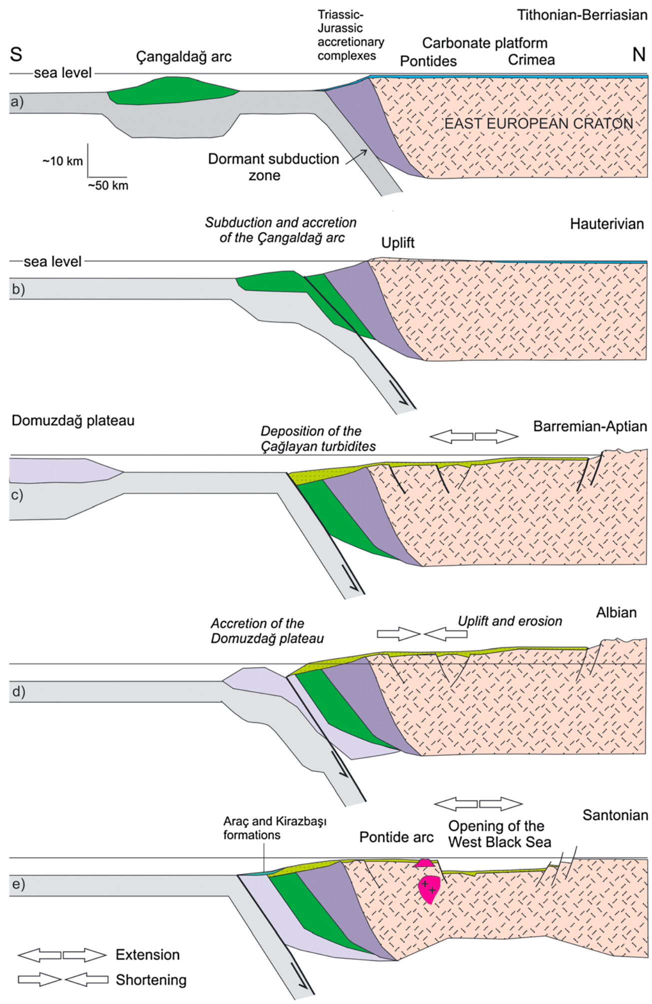

Figure 17. Schematic cross sections illustrating the Cretaceous evolution of the Eurasian margin.

metamorphic rocks of the Central Pontide Supercomplex. The Araç Formation can be compared with the Kirazbaşı Formation described from the Kargı Massif in the east (Figure 2). The Kirazbaşı Formation lies unconformably over the metamorphic rocks of the Domuzdağ Complex [*Yiğitbaş et al*., 1990; *Okay et al*., 2006; *Tüysüz and Tekin*, 2007]. It starts with basal pelagic limestones of Turonian-Santonian age, which are overlain by a flysch sequence. The flysch passes up into an ophiolitic mélange with tectonic slices and blocks of basalt, radiolarian chert, and serpentinite.

[48] The Araç and the Kirazbaşı formations represent basins developed in a fore-arc setting above accreted and metamorphosed trench sediments. The basalt and chert tectonic blocks must have been derived from the south from the uplifted segments of the accretionary complex. Chert blocks from the Kirazbaşı Formation yielded Middle Jurassic to Early Cretaceous radiolaria ages [*Tüysüz and Tekin*, 2007], which provide a minimum age span for the Tethyan ocean. The radiolarian cherts from ophiolitic mélange south of Araç have also recently been dated as Middle Jurassic [*Göncüoğlu et al*., 2012]. Continuing shortening in the fore-arc region led to the imbrication of the basin deposits with the underlying accretionary complex and subsequent folding. This last phase of major shortening is constrained between Santonian and Early Eocene.

8. Tectonic and Paleogeographic Evolution

8.1. Early Cretaceous (Hauterivian) Uplift: Response to Changes in Plate Movements

[49] During the latest Jurassic-earliest Cretaceous (Tithonian-Berriasian), an extensive shallow-marine carbonate platform covered the southern margin of the East European Craton including most of the Pontides, Moesia, Dobrugea, Crimea, and Caucasus [Figure 16a; e.g., *Görür*, 1988; *Altıner et al*., 1991; *Tari et al*., 1997; *Harbury and Cohen*, 1997; *Guo et al*., 2011; *Nikishin et al*., 2012). In the Eastern Pontides, this carbonate platform passed south to a passive margin dominated by pelagic limestone and calciturbidite with no evidence of ongoing subduction [*Okay and Şahintürk*, 1997]. As there is evidence for Triassic [*Okay and Monié*, 1997] and Jurassic [*Topuz et al*., 2013] subductions along the Pontide margin, the subduction zone must have become dormant during the latest Jurassic-earliest Cretaceous, when the movement of the Africa-Arabian plate with respect to Eurasia was a slow transform motion rather than convergence [*Rosenbaum et al*., 2002; *Smith*, 2006].

[50] The earliest Cretaceous carbonate deposition was followed by uplift and erosion in the platform areas of the Pontides during the Hauterivian, which exposed sequences

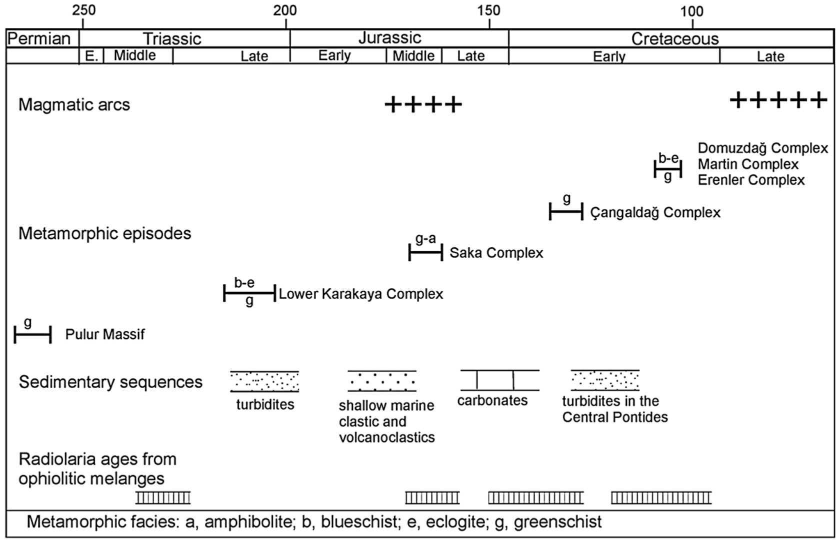

Figure 18. Metamorphic magmatic and major sedimentary episodes in the Sakarya Zone, Pontides. The metamorphic episodes are those of subduction-accretion complexes. The data for metamorphism are the following: Permian: *Topuz et al*. [2004]; Late Triassic: *Okay and Monié* [1997]; *Okay et al*. [2002]; Middle Jurassic: *Topuz et al*. [2013] and this study; Early Cretaceous: this study; Middle Cretaceous: *Okay et al*. [2006], *Akbayram et al*. [2013], and this study. The radiolaria age data are from *Tekin and Göncüoğlu* [2007, 2009] and *Tüysüz and Tekin* [2007]. The Jurassic arc magmatism is from *Meijers et al*. [2010b].

as old as the crystalline basement. A similar uplift and erosion is also recorded in the Crimea and in the Caucasus [*Mikhailov et al*., 1999; *Nikishin et al*., 2012]. In the Crimea, upper Barremian-Aptian deposits lie unconformably over rocks as old as the Triassic flysch [*Nikishin et al*., 2008].

[51] This is generally related to the rift-shoulder uplift preceding the opening of the Black Sea [e.g., *Görür*, 1988]. However, clastic zircon data from the Çağlayan Formation indicate that even as late as the Aptian, there was no thoroughgoing major rift separating the Central Pontides from the East European Craton. Furthermore, the Hauterivian uplift is very widespread and extends to the Eastern Pontides as well as to the rest of the Istanbul Zone. Thermochronological data indicate that Early Cretaceous uplift and erosion also took place in the northern part of the Ukranian shield northeast of Crimea [*Danišík et al*., 2008].

[52] We propose that the very broad and widespread Early Cretaceous (Hauterivian) uplift in the southern margin of the East European Craton is related to changes in the relative plate movements augmented with the collision of an ensimatic volcanic arc, the Çangaldağ Complex, with the Eurasian margin (Figure 17b). During the Early Cretaceous (Barremian, circa 125 Ma), the Africa-Arabian plate changed its motion with respect to Eurasia from slow sinistral transform motion to rapid convergence [e.g., *Smith*, 2006], which initially resulted in the buckling and uplift of the Eurasian margin. The subsequent activation of the dormant subduction zone was followed by the collision and underplating of the Çangaldağ volcanic arc, which was a further factor in the Hauterivian uplift (Figure 17b). The attempted subduction of oceanic plateaus or dormant ensimatic arcs produces uplift in the overriding plate, as observed in the Hikurangi-New Zealand subduction zone [e.g., *Davy et al*., 2009] and in numerical experiments [*Gerya et al*., 2009; *Tetreault and Buiter*, 2012].

8.2. Early Cretaceous (Barremian-Aptian) Rifting and Sedimentation

[53] During the Barremian-Aptian, the highland areas of Eurasia supplied clastic sediment to the south. Most of the Black Sea region, including Crimea, Caucasus, Dobrugea, and Moesia, was a platform with terrigeneous sedimentation [Figures 16b and 17c; e.g., *Harbury and Cohen*, 1997; *Adamia et al*., 2011; *Nikishin et al*., 2008; 2012]; only the western Sakarya Zone was the site of pelagic limestone deposition [*Altıner et al*., 1991]. There were two deep turbidite basins, one in the Central Pontides and the other in the Greater Caucasus. The sediments of the triangular-shaped Çağlayan turbidite basin was probably fed by a major river, which was draining the Ukranian shield south toward the Tethyan Ocean. An analogy is the present-day Nile river draining the interior of Africa into the oceanic East Mediterranean basin, which is slowly being subducted along the Cyprian arc [e.g., *Sestini*, 1989]. Syn-sedimentary normal faulting in the Çağlayan Formation and the presence of kilometer-size olistoliths indicate extension during the deposition of the Lower Cretaceous turbidites [*Tüysüz*, 1999; *Hippolyte et al*. 2012]. Subsidence is also recorded in the Crimea, where the water depth increased from 0 to 400–600 m between Barremian and Aptian [*Nikishin et al*., 2008]. The Karkinit basin in the Odessa shelf also started to open at this time [*Khriachtchevskaia et al*., 2010]. However, clastic zircon data suggest that there was no major thoroughgoing rift between Eurasia and the Pontides during the Barremian-Aptian; rather, extension was distributed over a large area. We relate the inception of the Barremian-Aptian extension in the Black Sea region to the establishment of a new subduction zone south of the accreted Çangaldağ Complex, which resulted in the relaxation and extension of the upper plate.

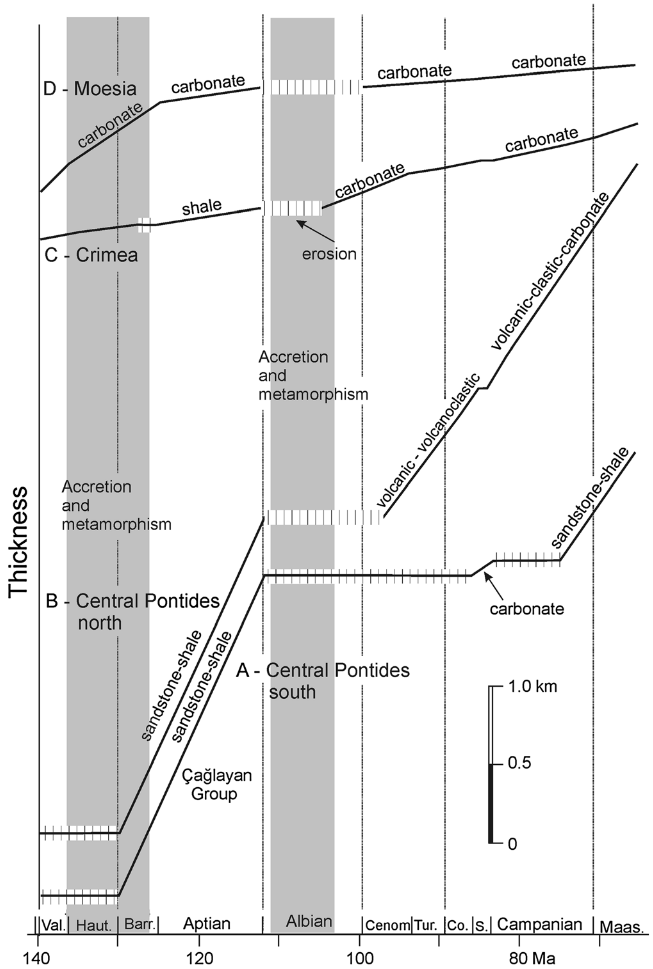

Figure 19. Thickness of the Cretaceous formations plotted against age for four regions around the Black Sea, where precise biostratigraphic and thickness data are available. (A and B) Fore-arc and volcanic arc regions of the Central Pontides, respectively [*Gedik and Korkmaz*, 1984; *Tüysüz*, 1999; *Leren et al.*, 2007]. (C) Bakhchisaray in southern Crimea [*Nikishin et al.*, 2008]. (D) Varna region in the Moesian Platform [*Harbury and Cohen*, 1997]. Note the general absence of the Albian strata and the much-reduced thickness in the platform areas compared to the Pontides. For locations of these areas, see Figure 1.

8.3. Early Cretaceous (Albian) Metamorphism and Uplift: Collision With an Oceanic Edifice

[54] Albian is characterized by widespread uplift in the Black Sea region (Figure 16c) and metamorphism in the Central Pontides. An accretionary complex with Albian (110 ± 3 Ma) metamorphic ages is also recently reported along the Intra-Pontide suture south of Istanbul [*Akbayram et al.*, 2013]. Albian uplift and erosion is also recorded in Crimea, where the uplift is estimated to be in the range of 400 to 800 m [*Nikishin et al.*, 2008] and extends west to the Moesian Platform [*Harbury and Cohen*, 1997] and east to the Eastern Pontides [*Robinson et al.*, 1995; *Okay and Şahintürk*, 1997], where the Albian strata are not recorded. Albian clastic sediments are only documented in the coastal areas of the western Central Pontides, in parts of the western Sakarya Zone [*Altıner et al.*, 1991] and Crimea [*Nikishin et al.*, 2008].

[55] The Ar-Ar ages indicate that a very large region in the Central Pontides, with a strike length of over 120 km and a structural thickness of over 20 km, underwent regional metamorphism in the Albian. Most of this tectonic pile consists of eclogite-facies and blueschist-facies rocks, a clear indication of subduction zone metamorphism. However, the age data do not show any directional pattern, as expected from a continuous subduction-accretion process but is clustered at around 107 Ma (Figure 5). Another unusual feature is that although there is clear evidence for subduction from the high-pressure metamorphism, a corresponding magmatic arc is missing. These features point to a singular event rather than steady state subduction-accretion for the underlying cause of the Albian orogeny. Along convergent margins, the collisions of topographic highs, such as oceanic islands or plateaus, result in uplift of the continental margin, a flat slab, and a lack of active volcanism [e.g., *von Huene and Ranero*, 2009]. We suggest that the Albian orogeny in the Pontides is caused by the collision and accretion of a large oceanic plateau, represented partly by the Domuzdağ Complex, with the Eurasian margin (Figures 16c and 17d).

8.4. Late Cretaceous Renewed Subsidence and Volcanism: Opening of the Black Sea Basin

[56] In the Late Cretaceous, the subduction zone jumped south of the accreted Domuzdağ Complex and this resulted in relaxation, extension, and subsidence of the upper plate (Figures 16d and 17c). The transgression started in the Central Pontides in the late Cenomanian in the north and reached the southern parts in the Santonian. It marked a change in the nature of sedimentation and is associated with the inception of arc volcanism. The Cenomanian-Santonian deposits are dominated by pelagic limestones, which are accompanied in the Black Sea coastal regions by submarine volcanic and volcaniclastic rocks. The earliest age for the Late Cretaceous volcanism in the Pontides is Turonian. The Turonian-Campanian Pontide volcanic arc, in places over 2000 m thick, never reached above the sea level. The submarine nature of the arc volcanism and scarcity of land-derived sediment indicate extension and subsidence during the Late Cretaceous in the Pontide margin of Eurasia. The Cenomanian to Paleocene period in Crimea, Dobrugea, and Moesia is also characterized by subsidence and deposition of limestone, sandy limestone, and chalk [*Harbury and Cohen*, 1997; *Nikishin et al.*, 2008]. This was the period of steady state subduction and regional extension. Both the rifting and the opening of the West Black Sea basin took place in the Cenomanian(?)-Turonian-Santonian [*Tüysüz*, 1999]. This view differs from the earlier models, in which rifting starts in the Barremian-Aptian and is followed 30 Myr later by the opening of the West Black Sea oceanic basin [e.g., *Görür*, 1988, 1997; *Okay et al.*, 1994; *Robinson et al.*, 1996; *Hippolyte et al.*, 2010]. The rifting of the back-arc basins takes place at the magmatic arc, which is the most ductile and weakest part of the system [e.g., *Karig*, 1970; *Tamaki*, 1985]. The lack of an Aptian-Albian magmatic arc, the absence of a thorough-going rift basin between the East European Craton and the Central Pontides during the Barremian-Aptian, and the widespread Albian uplift of the Black Sea region suggest that the Barremian-Aptian rifting and the Cenomanian(?)-Turonian-Santonian opening of the Western Black Sea basin are two distinct events separated

by the Albian uplift. In the models involving Barremian rifting and Turonian opening of the Black Sea, there is no explanation for the Albian regional uplift.

[57] Continental collision of the Pontide arc with the Kırşehir Block started at the end of the Cretaceous; by the end of the Eocene, the Pontides were above sea level [e.g., *Kaymakçı et al.*, 2009]. However, all of the metamorphism and most of the deformation in the southern part of the Central Pontides predate the early Tertiary arc-continent collision.

9. Pontides as a Long-Standing Active Margin of Eurasia

[58] The Pontides constituted the active margin of Eurasia at least since the Permian. Most of the Sakarya Zone consists of subduction-accretion complexes of Permian, Late Triassic, Middle Jurassic, and Early and middle Cretaceous ages (Figure 18). The addition of these metamorphosed subduction-accretion complexes has resulted in the southward growth of the Eurasian margin by at least 100 km. These subduction-accretion complexes consist predominantly of metabasic rocks, representing accreted oceanic plateaus or ensimatic arcs. The continental magmatic arcs are less well represented in the Pontides. There is good evidence only for Middle Jurassic [*Meijers et al.*, 2010b] and Late Cretaceous magmatic arcs. The abundance of Triassic zircons in the Lower Cretaceous turbidites suggests that a Triassic arc might be present under the Odessa shelf (Figure 1). However, no magmatic arc has developed in the Early Cretaceous, possibly because the subduction was new and/or the subducting slab was flat. During the Late Cretaceous, an extensional magmatic arc was formed above the subduction zone. The Late Cretaceous accretion was frontal and resulted in the formation of a thick accretionary complex made up of oceanic crustal lithologies. These ophiolitic mélanges were thrust south over the Anatolide-Tauride Block during the Maastrichtian-Early Eocene arc-continent collision and have a wide distribution in Anatolia. The determination of radiolaria in the ophiolitic mélanges has indicated a Middle Triassic to Cretaceous age range for the subducting Tethyan ocean [Figure 18; *Tekin and Göncüoğlu*, 2007, 2009; *Tüysüz and Tekin*, 2007]. The subduction was not continuous but was controlled by the relative motion of Africa-Arabian plate with respect to Eurasia. It became dormant during the Late Jurassic to earliest Cretaceous, when the motion was slow and transform type [*Smith*, 2006] and a major carbonate platform and a carbonate passive margin developed on the southern margin of Eurasia.

[59] A temporal correlation between the subduction-metamorphism-accretion episodes and the sedimentation patterns on the active margin and in the hinterland of Eurasia indicates that such episodes correspond to uplift and erosion in the upper plate. Figure 19 shows sedimentary thicknesses against age for four biostratigraphically well-constrained areas, two in the Pontides and two in the Eurasian hinterland. All four areas show uplift and erosion during the middle Cretaceous metamorphism (Figure 19). For the Early Cretaceous metamorphic event, the uplift is well documented in the Pontide margin but is less clear in the hinterland.

10. Conclusions

[60] 1. Changes in the plate motions and subduction of oceanic topographic highs are the primary controls in the sedimentation in the Eurasian margin and the Eurasian hinterland during the Cretaceous. The periods of extension-sedimentation and uplift-erosion are related to periods of steady state subduction and collision-accretion episodes, respectively. The collision-accretion episodes involve the clogging of the subduction zone by large oceanic edifices and are marked in the Central Pontides by accreted metamorphic complexes of Middle Jurassic (Bathonian-Callovian), Early Cretaceous (Hauterivian-Barremian), and middle Cretaceous (Albian) ages.

[61] 2. In the Central Pontides, Lower Cretaceous (Barremian-Aptian) submarine turbidites cover an area of 300 km by 60 km. Clastic zircon data from the turbiditic sandstones show that the East European Craton-Scythian Platform was likely to be a major source. This implies that there was no thoroughgoing Black Sea rift during the Early Cretaceous between the East European Craton and the Pontides, as shown in all paleogeographic reconstructions of the Black Sea region [e.g., *Robinson et al.*, 1996; *Barrier and Vrielynck*, 2008; *Nikishin et al.*, 2012].

[62] 3. A major problem encountered in petroleum exploration in the Black Sea has been the poor porosity and permeability of the sandstone reservoirs, which are generally sourced from the metamorphic and volcanic rocks of the Pontides [*Vincent et al.*, 2013]. In contrast, clastic zircons from the Çağlayan Formation indicate that the major source for the Lower Cretaceous sandstones was in the north in the granitoids and gneisses of the East European Craton rather than in the Pontides. Thus, suitable Lower Cretaceous sandstone reservoirs may exist at the Black Sea margins.

[63] 4. The southern distal parts of the Lower Cretaceous turbidites were deposited on the Tethyan oceanic crust and were subducted, metamorphosed, and underplated during the Early Cretaceous (Albian), as shown by the new U-Pb zircon and Ar-Ar ages.

[64] 5. The Lower Cretaceous turbidites in the southern part of the Central Pontides are strongly deformed with widespread folding and thrusting, which are usually ascribed to the Eocene and younger shortening. However, new data for the Early Cretaceous metamorphism and contractional deformation in the southern part of the Central Pontides suggest that a major part of this shortening is of Early Cretaceous (Albian) age.

[65] 6. The Albian metamorphism and deformation in the Central Pontides, and Albian regional uplift throughout the Black Sea region indicate that the Barremian-Aptian and the Cenomanian(?)-Turonian-Santonian represent two distinct periods of extension and sedimentation [*Tüysüz*, 1999]. The rifting and opening of the West Black Sea basin took place in the latter period, which also marks the beginning of Cretaceous arc volcanism in the Black Sea region.

[66] 7. The large area of metamorphic rocks in the Central Pontides south of the Lower Cretaceous turbidites, previously considered as Triassic or older basement, consists of Middle Jurassic and Early (Hauterivian-Barremian) and middle Cretaceous (Albian) metamorphic belts, as shown by the new Ar-Ar ages. They represent distinct subduction-accretion episodes in the southern active margin of Eurasia.

[67] 8. Models of the Paleo-Tethyan evolution in the Central Pontides invoke northward subduction of the Paleo-Tethys, creating an accretionary complex (Domuzdağ Complex) and a volcanic arc (the Çangaldağ Complex). The Triassic Küre back-arc basin opens up north of the volcanic arc [e.g., *Ustaömer and Robertson*, 1993, 1999]. According to these models, the back-arc system becomes inactive through the collision of a microcontinent, represented by the Kargı Massif. New isotopic data show that all these units, except the Küre Complex, are younger than Triassic. This annuls all the data for the back-arc origin of the Küre Complex. In terms of its age, lithology, and tectonic setting, the Küre Complex can be compared closely with the Upper Karakaya Complex, an Upper Triassic distal turbidite sequence deposited on the northern active margin of the Paleo-Tethys [e.g., *Okay and Göncüoğlu*, 2004].

[68] 9. The Pontides represent a segment of the Mesozoic active margin of Eurasia, which grew southward with the addition of Upper Triassic, Lower-Middle Jurassic, Lower Cretaceous, middle Cretaceous, and Upper Cretaceous accretionary complexes. It is an accretionary orogen, and its tectonic evolution is comparable to those of the North American Cordillera [e.g., *Dickinson*, 2009] and the Altaids in Central Asia [*Şengör et al.*, 1993].

[69] **Acknowledgments.** This study was supported by TÜBİTAK grant 109Y049 and partly by TÜBA. We thank Semih Can Ülgen and Remziye Akdoğan for help in the mineral separation, Christian Chopin for the use of the electron microprobe, Erkan Aydar and Evren Çubukçu for help with the cathodoluminescence images of zircons, Alison Halton and James Malley for help in analyzing the samples for Ar/Ar dating, and Ercan Özcan for the paleontological determinations of Eocene strata. S.J. Vincent and an anonymous reviewer are thanked for their detailed, comprehensive, and thoughtful comments, which improved the manuscript.

References

Adamia, S., G. Zakariadze, T. Chkhotua, N. Sadradze, N. Tsereteli, A. Chabukiani, and A. Gventsadze (2011), Geology of the Caucasus: A Review, *Turk. J. Earth Sci.*, *20*, 489–544.

Akbayram, K., A. I. Okay, and M. Satır (2013), Early Cretaceous closure of the Intra-Pontide Ocean in western Pontides (northwestern Turkey), *J. Geodyn.*, *65*, 38–55.

Aksay, A., Ş. Pehlivan, İ. Gedik, E. Bilginer, M. Duru, B. Akbaş, and İ. Altun (2002), Zonguldak sheet in the *Geological map series of Turkey*, scale 1: 500 000. Maden Tetkik ve Arama Genel Müdürlüğü, Ankara.

Alexandre, P., F. Chalot-Prat, A. Saintot, J. Wijbrans, R. Stephenson, M. Wilson, A. Kitchka, and S. Stovba (2004), The $^{40}Ar/^{39}Ar$ dating of magmatic activity in the Donbas Fold Belt and the Scythian Platform (Eastern European Craton), *Tectonics*, *23*, TC5002, doi:10.1029/2003TC001582.

Altıner, D., A. Koçyiğit, A. Farinacci, U. Nicosia, and M. A. Conti (1991), Jurassic-Lower Cretaceous stratigraphy and paleogeographic evolution of the southern part of north-western Anatolia, *Geol. Romana*, *28*, 13–80.

Aydın, M., H. S. Serdar, and Ö. Şahintürk (1982), The geology and the petroleum potential of the Central Black Sea region. Proceedings of the 6th Petroleum Congress of Turkey, Ankara, 63–71 (in Turkish).

Aydın, M., O. Demir, H. S. Serdar, S. Özaydın, and B. Harput (1995), Tectono-sedimentary evolution and hydrocarbon potential of Sinop-Boyabat basin, north Turkey, in *Geology of the Black Sea Region*, edited by A. Erler et al., pp. 254–263, MTA/JMO, Ankara.

Barrier, E., and B. Vrielynck (2008), MEBE Atlas of the Paleotectonic maps of the Middle East, *Commission for the Geological Map of the World*, Paris, France.

Boccaletti, M., P. Gocev, and P. Manetti (1974), Mesozoic isopic zones in the Black Sea region, *Societa Geologica Italiana Bollettino*, *93*, 547–565.

Bogdanova, S. V., B. Bingen, R. Gorbatschev, T. N. Kheraskova, V. I. Kozlov, V. N. Puchkov, and Y. A. Volozh (2008), The East European Craton (Baltica) before and during the assembly of Rodinia, *Precamb. Res.*, *160*, 23–45.

Bozkurt, E., J. A. Winchester, and M. Satır (2012), The Çele mafic complex: Evidence for Triassic collision between the Sakarya and Istanbul Zones, NW Turkey, *Tectonophysics*, *595-596*, 198–214.

Boztuğ, D. (1992), Lithostratigraphic units and tectonics of the southwestern part of Daday-Devrekani massif, western Pontides, Turkey, *Bull. Min. Res. Expl. Turkey*, *114*, 1–22.

Canca, N. (1994), 1:100 000 scale geological maps of the Western Black Sea coal basin. *Mineral Research and Exploration Institute of Turkey (MTA)*, Ankara.

Cavazza, C., I. Federici, A. I. Okay, and M. Zattin (2012), Apatite fission-track thermochronology of the Western Pontides (NW Turkey), *Geol. Mag.*, *149*, 133–140.

Çelik, Ö. F., A. Marzoli, R. Marschik, M. Chiaradia, F. Neubauer, and İ. Öz (2011), Early–Middle Jurassic intra-oceanic subduction in the İzmir-Ankara-Erzincan Ocean, Northern Turkey, *Tectonophysics*, *539*, 120–134.

Channel, J. E. T., O. Tüysüz, O. Bektas, and A. M. C. Şengör (1996), Jurassic-Cretaceous paleomagnetism and paleogeography of the Pontides (Turkey), *Tectonics*, *15*, 201–212.

Chen, F., W. Siebel, M. Satır, N. Terzioğlu, and K. Saka (2002), Geochronology of the Karadere basement (NW Turkey) and implications for the geological evolution of the Istanbul Zone, *Int. J. Earth Sci.*, *91*, 469–481.

Claesson, S., E. Bibikova, S. Bogdanova, and V. Skobelev (2006), Archean terranes, Paleoproterozoic reworking and accretion in the Ukranian Shield, East European Craton, in *European Lithosphere Dynamics*, vol. 32, edited by D. G. Gee and R. A. Stephenson, pp. 645–654, Geological Society, London, Memoirs, Oxford, UK.

Danišík, M., R. F. Sachsenhofer, V. A. Privalov, E. A. Panova, W. Frisch, and C. Spiegel (2008), Low-temperature thermal evolution of the Azov Massif (Ukrainian Shield–Ukraine) — Implications for interpreting (U–Th)/He and fission track ages from cratons, *Tectonophysics*, *456*, 171–179.

Davy, B., H. Kaj, and W. Reinhard (2009), Hikurangi Plateau: Crustal structure, rifted formation, and Gondwana subduction history, *Geochem. Geophys. Geosyst.*, *9*, Q07004, doi:10.1029/2007GC001855.

Dean, W. T., O. Monod, R. B. Rickards, O. Demir, and P. Bultynck (2000), Lower Palaeozoic stratigraphy and palaeontology, Karadere-Zirze area, Pontus Mountains, northern Turkey, *Geol. Mag.*, *137*, 555–582.

Derman, A. S. (2002), Black Sea rift sequences, *Türkiye Petrol Jeologları Derneği Bülteni*, *14*, 36–65.

Derman, A. S., and Y. H. İztan (1997), Results of geochemical analysis of seeps and potential source rocks from northern Turkey and the Turkish Black Sea, in *Regional and Petroleum Geology of the Black Sea and Surrounding Region*, vol. 68, edited by A. G. Robinson, pp. 313–330, American Association of Petroleum Geologists Memoir, Tulsa, Oklahoma.

Dickinson, W. R. (2009), Anatomy and global context of the North American Cordillera, in *Backbone of the Americas: Shallow Subduction, Plateau Uplift, and Ridge and Terrane Collision*, vol. 204, edited by S. M. Kay et al., pp. 1–29, Geological Society of America Memoir, Denver, USA, doi:10.1130/2009.1204.

Enay, R. (1976), Faunes Anatoliennes (Ammonitina, Jurassique) et domaines biogéographiques nord et sud Téthysiens, *Bull. Soc. Geol. Fr.*, *7*(18), 533–541.

Evans, B. W. (1990), Phase relations of epidote-blueschists, *Lithos*, *25*, 3–23.

Gedik, A., and S. Korkmaz (1984), Geology and petroleum potential of the Sinop basin, *Jeoloji Mühendisliği*, *19*, 53–79 (in Turkish).

Gerya, T. V., D. Fossati, C. Cantieni, and D. Seward (2009), Dynamic effects of aseismic ridge subduction: Numerical modelling, *Eur. J. Mineral.*, *21*, 649–661.

Göncüoğlu, M. C., M. Marroni, K. Sayit, U. K. Tekin, G. Ottria, L. Pandolfi, and A. Ellero (2012), The Ayli Dag ophiolite sequence (central-northern Turkey): A fragment of Middle Jurassic oceanic lithosphere within the Intra-Pontide suture zone, *Ofioliti*, *37*, 77–92.

Görür, N. (1988), Timing of opening of the Black Sea basin, *Tectonophysics*, *147*, 247–262.

Görür, N. (1997), Cretaceous syn- to postrift sedimentation on the southern continental margin of the western Black Sea Basin, in *Regional and Petroleum Geology of the Black Sea and Surrounding Region*, vol. 68, edited by A. G. Robinson, pp. 227–240, American Association of Petroleum Geologists Memoir, Tulsa, Oklahoma.

Görür, N., and O. Tüysüz (1997), Petroleum geology of the southern continental margin of the Black Sea, in *Regional and Petroleum Geology of the Black Sea and Surrounding Region*, vol. 68, edited by A. G. Robinson, pp. 241–254, American Association of Petroleum Geologists Memoir, Tulsa, Oklahoma.

Görür, N., O. Tüysüz, A. Aykol, M. Sakınç, E. Yiğitbaş, and R. Akkök (1993), Cretaceous red pelagic carbonates of northern Turkey - their place in the opening history of the Black-Sea, *Eclog. Geol. Helv.*, *86*, 819–838.

Gradstein, F. M., J. G. Ogg, and A. G. Smith (2004), *A Geologic Time Scale 2004*, Cambridge Univ. Press, Cambridge.

Guo, L., S. J. Vincent, and V. Lavrishchev (2011), Upper Jurassic reefs from the Russian western Caucasus: Implications for the eastern Black Sea, *Turk. J. Earth Sci.*, *20*, 629–653.

Harbury, N., and M. Cohen (1997), Sedimentary history of the Late Jurassic-Paleogene of northeast Bulgaria and the Bulgarian Black Sea, in *Regional and Petroleum Geology of the Black Sea and Surrounding Region*, vol. 68, edited by A. G. Robinson, pp. 129–168, American Association of Petroleum Geologists Memoir, Tulsa, Oklahoma.

Hippolyte, J.-C., C. Müller, N. Kaymakçı, and E. Sangu (2010), Dating of the Black Sea Basin: New nannoplankton ages from its inverted margin in the Central Pontides (Turkey), in *Sedimentary Basin Tectonics from the Black Sea and Caucasus to the Arabian Platform*, vol. 340, edited by R. A. Stephenson et al., pp. 113–136, Geological Society, London, Special Publication.

Hippolyte, J.-C., N. Kaymakçı, E. Sangu, C. Müller, and N. Espurt (2012), Structural and paleostress evolution of the Pontides from the rifting of the Black Sea basin to the inception of the North Anatolian Fault, *Abstracts Book*, 65th Geol. Congress of Turkey, Ankara, pp. 60–61.

Holland, T. J. B., and R. Powell (1998), An internally consistent thermodynamic data set for phases of petrological interest, *J. Metamorphic Geol.*, *16*, 309–343.

Karig, D. E. (1970), Ridges and basins of the Tonga-Kermadac island arc system, *J. Geophys. Res.*, *75*, 239–254.

Karslıoğlu, Ö., T. Ustaömer, A. H. F. Robertson, and I. Peytcheva (2012), Age and provenance of detrital zircons from a sandstone turbidite of the Triassic-Early Jurassic Küre Complex, Central Pontides, N Turkey, *Int. Earth Science Colloquium on the Aegean region, IESCA-2012*, Abstract Book, p. 57.

Kaymakçı, N., Y. Özçelik¸ S. H. White, and P. M. van Dijk (2009), Tectonostratigraphy of the Çankırı Basin: Late Cretaceous to early Miocene evolution of the Neotethyan Suture Zone in Turkey, in *Collision and Collapse at the Africa–Arabia–Eurasia Subduction Zone*, vol. 311, edited by D. J. J. van Hinsbergen et al., pp. 67–106, Geological Society, London, Special Publication, Oxford, UK.

Kennedy, W. J., C. Tunoğlu, I. Walaszczyk, and İ. K. Ertekin (2007), Ammonite and inoceramid bivalve faunas from the Davutlar Formation of the Devrekani-Kastamonu area, northern Turkey, and their biostratigraphical significance, *Cretaceous Res.*, *28*, 861–894.

Khriachtchevskaia, O., S. Stovba, and R. Stephenson (2010), Cretaceous-Neogene tectonic evolution of the northern margin of the Black Sea from seismic reflection data and tectonic subsidence analysis, in *Sedimentary Basin Tectonics from the Black Sea and Caucasus to the Arabian Platform*, vol. 340, edited by M. Sosson et al., pp. 137–157, Geological Society, London, Special Publication, Oxford, UK.

Korkmaz, S. (1992), A new approach to source rock facies, organic maturation and oil generation in the Sinop basin from the point of volcanism and depositional environment, *Türkiye Petrol Jeologları Derneği Bülteni*, *4*, 35–45 (in Turkish).

Leren, B. L. S., N. E. Janbu, W. Nemec, E. Kırman, and A. Ilgar (2007), Late Cretaceous to early Eocene sedimentation in the Sinop-Boyabat Basin, north-central Turkey: a deep-water turbiditic system evolving into littoral carbonate platform, in *Sedimentary Processes, Environments and Basins*, International Association of Sedimentologists Special Publication, vol. 38, edited by G. Nichols et al., pp. 401–457, Blackwell Publishing, Oxford, UK.

Masse, J.-P., O. Tüysüz, M. Fenerci-Masse, S. Özer, and B. Sarı (2009), Stratigraphic organisation, spatial distribution, palaeoenvironmental reconstruction, and demise of Lower Cretaceous (Barremian-lower Aptian) carbonate platforms of the Western Pontides (Black Sea region, Turkey), *Cretaceous Res.*, *30*, 1170–1180.

Meijers, M. J. M., N. Kaymakci, D. J. J. van Hinsbergen, C. G. Langereis, R. A. Stephenson, and J.-C. Hippolyte (2010a), Late Cretaceous to Paleocene oroclinal bending in the central Pontides (Turkey), *Tectonics*, *29*, TC4016, doi:10.1029/2009TC002620.

Meijers, M. J. M., B. Vrouwe, D. J. J. van Hinsbergen, K. F. Kuiper, J. Wijbrans, G. R. Davies, R. A. Stephenson, N. Kaymakcı, L. Matenco, and A. Saintot (2010b), Jurassic arc volcanism on Crimea (Ukraine): Implications for the paleo-subduction zone configuration of the Black Sea region, *Lithos*, *119*, 412–426.

Mikhailov, V. O., L. V. Panina, R. Polino, N. V. Koronovsky, E. A. Kiseleva, N. V. Klavdieva, and E. I. Smolyaninova (1999), Evolution of the North Caucasus foredeep: Constraints based on the analysis of subsidence curves, *Tectonophysics*, *307*, 361–379.

Nikishin, A. M., A. S. Alekseev, E. J. Baraboshkin, L. F. Kopaevich, R. R. Gabdullin, and N. V. Badulina (2008), The Cretaceous history of the Bakhchisaray area, southen Crimea (Ukraine), *Bulletin De L Institut Royal Des Sciences Naturelles De Belgique-Sciences De La Terre*, *78*, 75–85.

Nikishin, A., P. Ziegler, S. Bolotov, and P. Fokin (2012), Late Palaeozoic to Cenozoic Evolution of the Black Sea-Southern Eastern Europe Region: A View from the Russian Platform, *Turk. J. Earth Sci.*, *21*, 571–634.

Nzegge, O. M., M. Satir, W. Siebel, and H. Taubald (2006), Geochemical and isotopic constraints on the genesis of the Late Palaeozoic Deliktas¸ and Sivrikaya granites from the Kastamonu granitoid belt (Central Pontides, Turkey), *N. Jb. Miner. Abh.*, *183*, 27–40.

Okay, A. I., and M. C. Göncüoğlu (2004), Karakaya Complex: A review of data and concepts, *Turk. J. Earth Sci.*, *13*, 77–95.

Okay, A. I., and P. Monié (1997), Early Mesozoic subduction in the Eastern Mediterranean: Evidence from Triassic eclogite in northwest Turkey, *Geology*, *25*, 595–598.

Okay, A. I., and Ö. Şahintürk (1997), Geology of the Eastern Pontides, in *Regional and Petroleum Geology of the Black Sea and Surrounding Region*, vol. 68, edited by A. G. Robinson, pp. 291–311, American Association of Petroleum Geologists Memoir, Tulsa, Oklahoma.

Okay, A. I., and O. Tüysüz (1999), Tethyan sutures of northern Turkey, in *The Mediterranean Basins: Tertiary Extension Within the Alpine Orogen*, vol. 156, edited by B. Durand et al., pp. 475–515, Geological Society, London, Special Publication, Oxford, UK.

Okay, A. I., A. M. C. Şengör, and N. Görür (1994), Kinematic history of the opening of the Black Sea and its effects on the surrounding regions, *Geology*, *22*, 267–270.

Okay, A. I., M. Satır, O. Tüysüz, S. Akyüz, and F. Chen (2001), The tectonics of the Strandja Massif: Variscan and mid-Mesozoic deformation and metamorphism in the northern Aegean, *Int. J. Earth Sci.*, *90*, 217–233.

Okay, A. I., O. Monod, and P. Monié (2002), Triassic blueschists and eclogites from northwest Turkey: Vestiges of the Paleo-Tethyan subduction, *Lithos*, *64*, 155–178.

Okay, A. I., O. Tüysüz, M. Satır, S. Özkan-Altıner, D. Altıner, S. Sherlock, and R. H. Eren (2006), Cretaceous and Triassic subduction-accretion, HP/LT metamorphism and continental growth in the Central Pontides, Turkey, *Geol. Soc. Am. Bull.*, *118*, 1247–1269.

Okay, N., T. Zack, A. I. Okay, and M. Barth (2010), Sinistral transport along the Trans-European Suture Zone: Detrital zircon-rutile geochronology and sandstone petrography from the Carboniferous flysch of the Pontides, *Geol. Mag.*, *148*, 380–403.

Özcan, E., G. Less, and B. Kertesz (2007), Late Ypresian to middle Lutetian Orthophragminid record from central and northern Turkey: Taxonomy and remarks on zonal scheme, *Turk. J. Earth Sci.*, *16*, 281–318.

Powell, R., and T. J. B. Holland (1988), An internally consistent thermodynamic dataset with uncertainties and correlations: 3. Application methods, worked examples and a computer program, *J. Metamorphic Geol.*, *6*, 173–204.

Robinson, A. G., C. J. Banks, M. M. Rutherford, and J. P. P. Hirst (1995), Stratigraphic and structural development of the Eastern Pontides, Turkey, *J. Geol. Soc. London*, *152*, 861–872.

Robinson, A. G., J. H. Rudat, C. J. Banks, and R. L. F. Wiles (1996), Petroleum geology of the Black Sea, *Marine and Petroleum Geol.*, *13*, 195–223.

Rojay, B., and D. Altıner (1998), Middle Jurassic-Lower Cretaceous biostratigraphy in the Central Pontides (Turkey): Remarks on paleogeography and tectonic evolution, *Rivista It. Paleont. Strat.*, *104*, 167–180.

Rosenbaum, G., G. S. Lister, and C. Duboz (2002), Relative motions of Africa, Iberia and Europe during Alpine orogeny, *Tectonophysics*, *359*, 117–129.

Safonova, I., S. Maruyama, T. Hirata, Y. Kon, and S. Rino (2010), LA ICP MS U–Pb ages of detrital zircons from Russia largest rivers: Implications for major granitoid events in Eurasia and global episodes of supercontinent formation, *J. Geodynamics*, *50*, 134–153.

Şen, Ş. (2013), New evidences for the formation of and for petroleum exploration in the fold-thrust zones of the central Black Sea Basin of Turkey, *Am. Assoc. Petrol. Geol. Bull.*, *97*, 465–485.

Şengör, A. M. C., and Y. Yılmaz (1981), Tethyan evolution of Turkey: A plate tectonic approach, *Tectonophysics*, *75*, 181–241.

Şengör, A. M. C., Y. Yılmaz, and İ. Ketin (1980), Remnants of a pre-late Jurassic ocean in northern Turkey: Fragments of Permo-Triassic Paleo-Tethys?, *Geol. Soc. Am. Bull.*, *91*, 599–609.

Şengör, A. M. C., Y. Yılmaz, and O. Sungurlu (1984), Tectonics of the Mediterranean Cimmerides: nature and evolution of the western termination of Palaeo-Tethys, in *Geological Evolution of the Eastern Mediterranean*, vol. 17, edited by J. E. Dixon and A. H. F. Robertson, pp. 77–112, Geological Society, London, Special Publication, Oxford, UK.

Şengör, A. M. C., B. A. Natal'in, and V. S. Burtman (1993), Evolution of the Altaid tectonic collage and Palaeozoic crustal growth in Eurasia, *Nature*, *364*, 299–307.

Sestini, G. (1989), Nile Delta: A review of depositional environments and geological history, in *Deltas: Sites and Traps for Fossil Fuels*, Geological Society, London, Special Publication, vol. 41, edited by M. K. G. Whateley and K. T. Pickering, pp. 99–127, Oxford, UK.

Smith, A. G. (2006), Tethyan ophiolite emplacement, Africa to Europe motions, and Atlantic spreading, in *Tectonic development of the Eastern Mediterranean Region*, vol. 200, edited by A. H. F. Robertson and D. Mountrakis, pp. 11–34, Geological Society, London, Special Publication, Oxford, UK.

Somin, M. (2011), Pre-Jurassic basement of the Greater Caucasus: brief overview, *Turk. J. Earth Sci.*, *20*, 545–610.

Sunal, G., and O. Tüysüz (2002), Palaeostress analysis of Tertiary postcollisional structures in the western Pontides, northern Turkey, *Geol. Mag.*, *139*, 343–359, doi:10.1017/S0016756802006489.

Sunal, G., B. Natal'in, M. Satır, and E. Toraman (2006), Paleozoic magmatic events in the Strandja Masif, NW Turkey, *Geodinamica Acta*, *19*, 283–300.

Tamaki, K. (1985), Two modes of back-arc spreading, *Geology*, *13*, 475–478.

Tari, G., O. Dicea, J. Faulkerson, G. Georgiev, S. Popov, M. Stefanescu, and G. Weir (1997), Cimmerian and Alpine stratigraphy and structural evolution of the Moesian Platform (Romania/Bulgaria), in *Regional and Petroleum Geology of the Black Sea and Surrounding Region*, vol. 68, edited by A. G. Robinson, pp. 63–90, American Association of Petroleum Geologists Memoir, Tulsa, Oklahoma.

Tekin, U. K., and M. C. Göncüoğlu (2007), Discovery of the oldest (Upper Ladinian to Middle Carnian) radiolarian assemblages from the Bornova Flysch Zone in western Turkey: Implications for the evolution of the Neotethyan Izmir-Ankara ocean, *Ofioliti*, *32*, 131–150.

Tekin, U. K., and M. C. Göncüoğlu (2009), Late Middle Jurassic (Late Bathonian-Early Callovian) radiolarian cherts from the Neotethyan Bornova Flysch Zone, Spil Mountains, Western Turkey, *Stratigr. Geol. Correl.*, *17*, 298–308.

Tetreault, J. L., and S. J. H. Buiter (2012), Geodynamic models of terrane accretion: Testing the fate of island arcs, oceanic plateaus, and continental fragments in subduction zones, *J. Geophys. Res.*, *117*, B08403, doi:10.1029/2012JB009316.

Topuz, G., R. Altherr, M. Satir, and W. H. Schwartz (2004), Low-grade metamorphic rocks from the Pulur Complex, NE Turkey: Implications for the pre-Liassic evolution of the Eastern Pontides, *Int. J. Earth Sci.*, *93*, 72–91.

Topuz, G., G. Göçmengil, Y. Rolland, Ö. F. Çelik, T. Zack, and A. K. Schmitt (2013), Jurassic accretionary complex and ophiolite from northeast Turkey: No evidence for the Cimmerian continental ribbon, *Geology*, *41*, 255–258.

Tunoğlu, C. (1991), Microfacies analysis of the Upper Jurassic – Lower Cretaceous carbonate sequence of Devrekani basin (north Kastamonu), *Türkiye Petrol Jeologları Derneği Bülteni*, *3*, 75–86 (in Turkish).

Tüysüz, O. (1990), Tectonic evolution of a part of the Tethyside orogenic collage: The Kargı Massif, northern Turkey, *Tectonics*, *9*, 141–160.

Tüysüz, O. (1999), Geology of the Cretaceous sedimentary basins of the Western Pontides, *Geol. J.*, *34*, 75–93.

Tüysüz, O., and U. K. Tekin (2007), Timing of imbrication of an active continental margin facing the northern branch of Neotethys, *Kargı Massif, northern Turkey, Cretaceous Res.*, *28*, 754–764.

Tüysüz, O., and E. Yiğitbaş (1994), The Karakaya basin: a Palaeo-Tethyan marginal basin and its age of opening, *Acta Geologica Hungarica*, *37*, 327–350.

Tüysüz, O., İ. Ö. Yılmaz, L. Švábenická, and S. Kirici (2012), The Unaz Formation: A Key Unit in the Western Black Sea Region, N Turkey, *Turk. J. Earth Sci.*, *21*, 1009–1028.

Uğuz, M. F., M. Sevin, M. Duru, (2002), Sinop sheet in the *Geological map series of Turkey*, scale 1: 500 000, Maden Tetkik ve Arama Genel Müdürlüğü, Ankara.

Ustaömer, T., and A. H. F. Robertson (1993), A Late Paleozoic-Early Mesozoic marginal basin along the active southern continental margin of Eurasia: Evidence from the Central Pontides (Turkey) and adjacent regions, *Geol. J.*, *28*, 219–238.

Ustaömer, T., and A. H. F. Robertson (1994), Late Paleozoic marginal basin and subduction-accretion: the Paleotethyan Küre Complex, Central Pontides, northern Turkey, *J. Geol. Soc. London*, *151*, 291–305.

Ustaömer, T., and A. H. F. Robertson (1997), Tectonic-sedimentary evolution of the North-Tethyan margin in the Central Pontides of northern Turkey, in *Regional and Petroleum Geology of the Black Sea and Surrounding Region*, vol. 68, edited by A. G. Robinson, pp. 255–290, American Association of Petroleum Geologists Memoir, Tulsa, Oklahoma.

Ustaömer, T., and A. H. F. Robertson (1999), Geochemical evidence used to test alternative plate tectonic models for the pre-Upper Jurassic (Palaeotethyan) units in the Central Pontides, N Turkey, *Geol. J.*, *34*, 25–53.

Ustaömer, P. A., R. Mundil, and P. R. Renne (2005), U/Pb and Pb/Pb zircon ages for arc-related intrusions of the Bolu Massif (W Pontides, NW Turkey): Evidence for Late Precambrian (Cadomian) age, *Terra Nova*, *17*, 215–223.

Ustaömer, P. A., T. Ustaömer, A. Gerdes, and G. Zulauf (2011), Detrital zircon ages from a Lower Ordovician quartzite of the Istanbul exotic terrane (NW Turkey): Evidence for Amazonian affinity, *Int. J. Earth Sci.*, *100*, 23–41.

Vincent, S. J., A. C. Morton, F. Hyden, and M. Fanning (2013), Insights from petrography, mineralogy and U-Pb zircon geochronology into the provenance and reservoir potential of Cenozoic siliciclastic depositional systems supplying the northern margin of the Eastern Black Sea, *Mar. Pet. Geol.*, *45*, 331–348, doi:10.1016/j.marpetgeo.2013.04.002, in press.

von Huene, R., and C. R. Ranero (2009), Neogene collision and deformation of convergent margins along the backbone of the Americas, in *Backbone of the Americas: Shallow Subduction, Plateau Uplift, and Ridge and Terrane Collision*, vol. 204, edited by S. M. Kay et al., pp. 67–83, Geological Society of America Memoir, Denver, USA.

Wang, C. Y., I. H. Campbell, A. S. Stepanov, C. M. Allen, and I. N. Burtsev (2011), Growth rate of the preserved continental crust: II. Constraints from Hf and O isotopes in detrital zircons from Greater Russian Rivers, *Geochim. Cosmochim. Acta*, *75*, 1308–1345.

Yardley, B. W. D. (1989), *An Introduction to Metamorphic Petrology*, Longman Scientific & Technical, New York.

Yiğitbaş, E., O. Tüysüz, and H. S. Serdar (1990), Geological features of the Late cretaceous active continental margin of the Central Pontides, Proceedings of the 8th Petroleum Congress of Turkey, Ankara, 141–151 (in Turkish).

Yiğitbaş, E., A. Elmas, and Y. Yılmaz (1999), Pre-Cenozoic tectonostratigraphic components of the western Pontides and their geological evolution, *Geol. J.*, *34*, 55–74.

Yılmaz, İ. (1975), Determination de l'age d'un granite de Sancaktepe, dans la presquile de Kocaeli (Nord de la Mer de Marmara), *C.R.Ac. Sci. D 281*, 1563–1565, Paris.

Yılmaz, O. (1980), Lithostratigraphic units and tectonics of the northeastern part of the Daday-Devrakani Massif, *Yerbilimleri*, *5-6*, 101–135, (in Turkish).

Yılmaz, O. (1988), L'ensemble ophiolitique de Çangal (Turquie du Nord): Mise en évidence d'un métamorphisme océanique et d'un rétrométamorphisme cataclastique tardif, *Geologie Alpine*, *64*, 113–132.

Yılmaz, İ. Ö., and D. Altıner (2007), Cyclostratigraphy and sequence boundaries of inner platform mixed carbonate-siliciclastic successions (Barremian-Aptian) (Zonguldak, NW Turkey), *J. Asian Earth Sci.*, *30*, 253–270.

Yılmaz, O., and D. Boztuğ (1986), Kastamonu granitoid belt of northern Turkey: First arc plutonism product related to the subduction of the Paleo-Tethys, *Geology*, *14*, 179–183.

Yılmaz, Y., and A. M. C. Şengör (1985), Palaeo-Tethyan ophiolites in northern Turkey: Petrology and tectonic setting, *Ofioliti*, *10*, 485–504.

Yılmaz, O., D. Boztuğ, and M. G. Bonhomme (1997a), The existence of the Early to Middle Jurassic and Early Cretaceous metamorphic episodes obtained by K-Ar geochronology in the Daday- Devrekani Massif and surroundings, Kastamonu Region, Northern Turkey, *İ. Ü. Müh. Fak. Yerbilimleri Dergisi*, *10*, 95–109.

Yılmaz, Y., O. Tüysüz, E. Yiğitbaş, C. Ş. Genç, and A. M. C. Şengör (1997b), Geology and tectonic evolution of the Pontides, in *Regional and Petroleum Geology of the Black Sea and Surrounding Region*, vol. 68, edited by A. G. Robinson, pp. 183–226, American Association of Petroleum Geologists Memoir, Tulsa, Oklahoma.

Yılmaz, İ. Ö., D. Altıner, U. K. Tekin, O. Tüysüz, F. Ocakoğlu, and S. Açıkalın (2010), Cenomanian – Turonian Oceanic Anoxic Event (OAE2) in the Sakarya Zone, northwestern Turkey: Sedimentological, cyclostratigraphic, and geochemical records, *Cretaceous Res.*, *31*, 207–226.

Zonenshain, L. P., and X. Lepichon (1986), Deep basins of the Black-Sea and Caspian Sea as remnants of Mesozoic back-arc basins, *Tectonophysics*, *123*, 181–211.